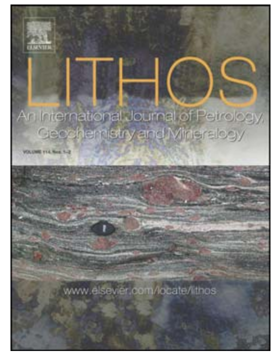

Early Eocene clinoenstatite boninite and boninite-series dikes of the ophiolite of New Caledonia; a witness of slab-derived enrichment of the mantle wedge in a nascent volcanic arc

Dominique Cluzel, Marc Ulrich, Fred Jourdan, Sebastien Meffre, Jean-Louis Paquette, Marc-Antoine Audet, Arianna Secchiari, Pierre Maurizot

PII: S0024-4937(16)30066-4
DOI: doi: 10.1016/j.lithos.2016.04.031
Reference: LITHOS 3917

To appear in: *LITHOS*

Received date: 6 February 2016
Accepted date: 29 April 2016

Early Eocene clinoenstatite boninite and boninite-series dikes of the ophiolite of New Caledonia; a witness of slab-derived enrichment of the mantle wedge in a nascent volcanic arc.

Dominique Cluzel[1], Marc Ulrich[2], Fred Jourdan[3], Sebastien Meffre[4], Jean-Louis Paquette[5], Marc-Antoine Audet[6], Arianna Secchiari[7] and Pierre Maurizot[8]

[1] Université de la Nouvelle-Calédonie, BP R4, 98851 Nouméa Cedex, New Caledonia, (dominique.cluzel@univ-nc.nc)

[2] Université de Strasbourg, - IPGS-EOST, 1 rue Blessig, 67084 Strasbourg-Cedex (mulrich@unistra.fr)

[3] Western Australian Argon Isotope Facility. Department of Applied Geology and JdL Centre, Curtin University of Technology. GPO Box U1987 Perth, WA 6845. (F.Jourdan@exchange.curtin.edu.au)

[4] University of Tasmania, Private Bag 79, Hobart 7001, Australia (smeffre@utas.edu.au)

[5] Université Blaise Pascal, UMR 6524 Magmas et Volcans, 34 Avenue Carnot, 63000 Clermont-Ferrand, France (J.L.paquette@opgc.univ-bpclermont.fr)

[6] Sama Resources Inc. 1055 West Hastings Street, Vancouver, BC V6E 2E9, Canada (marc-antoine257@hotmail.com)

[7] Università di Parma, Dipartimento di Fisica e Scienze della Terra "Macedonio Melloni" Parco Area delle Scienze, 7/A Parma, Italia (arianna.secchiari@nemo.unipr.it)

[8] Service Géologique de la Nouvelle-Calédonie, DIMENC B.P. 465, 98845 Nouméa, New Caledonia. (pierre.maurizot@gouv.nc)

Abstract

Clinoenstatite-bearing boninites (CE-boninite) from the serpentinite sole of the Cenozoic ophiolite of New Caledonia near Nepoui have been dated by the $^{40}Ar/^{39}Ar$ method, yielding two plateau ages of 47.4 ± 0.9 Ma and 50.4 ± 1.3 Ma. Coarser grained, geochemically similar boninite-series felsic dikes consistently yielded U-Pb zircon ages of ca. 54 Ma.

Nepoui CE-boninites display whole rock geochemical features similar to that of Cape Vogel boninites (Papua-New Guinea). They similarly have been generated by low degree hydrous melting of depleted peridotite. High contents in LILE and LREE, and some elemental ratios suggest source enrichment by subduction-derived fluids and melts. However, unlike the Cape Vogel boninite, moderately depleted MORB-like isotopic signatures (εNd_{50} = 7.9) rule out the role of OIB-like, or E-MORB component that might account for the relatively high LREE and LILE contents measured in the rocks. Nd isotopic ratios and positive anomalies in Zr and Hf are closely similar to that of the slightly older felsic dikes (55-50 Ma) that crosscut the peridotite from the ophiolite in New Caledonia. Most of these magmas have been generated by slab melting during the early stages of intra-oceanic subduction. The Early Eocene subduction started at or near the “oceanic” ridge and involved young and hot lithosphere; therefore, slab-derived melts may have reacted locally with hot depleted peridotites. Finally, water influx into the mantle wedge during the subduction of slightly older (cooler and hydrated) lithosphere initiated a low degree partial melting event in the mantle wedge and generated the CE-boninite magma.

Geochemical modeling of hydrous melting of a depleted mantle re-enriched by slab melts suggest that the additional slab melt component was derived from the partial melting of a BABB-like barroisite-bearing eclogite, similar to some elements of the Eocene HP-LT Pouebo terrane. This potential magma source is similar to the BABB-like HT amphibolites of the metamorphic sole of the ophiolite, which have the same origin. Geochemical modeling also suggests that CE-boninite magma may have been in equilibrium with the enstatite-bearing gabbro cumulates that crop out in several places of the Massif du Sud.

However, modeling fails in establishing that harzburgite of the same massif simply corresponds to the melting residue of this process. It appears that ultra-depleted supra-subduction peridotites of the Massif du Sud are probably not directly related to the overlying gabbro cumulates.

Keywords: Supra-subduction ophiolite, fore-arc, clinoenstatite boninite, leucodiorite, subduction inception, REE, fluids, slab melt

Introduction

Boninites are supra-subduction high-Mg volcanic rocks (SiO_2>52 wt %, MgO>8 wt %, and TiO_2<0.5 wt %). They can be divided into low-Ca (CaO/Al_2O_3<0.5) and high-Ca (0.7<CaO/Al_2O_3<1.0) series based on their bulk major element compositions (Crawford et al., 1989). Previous studies have suggested that boninite magmas can be generated from low-pressure hydrous partial melting of depleted mantle in anomalously hot mantle wedges. However, influx of subduction-derived fluids alone cannot account for all the geochemical features of boninites, which generally display high contents of large ion lithophile elements (LILE) and light rare earth elements (LREE) compared with their potential source rocks. Therefore, source enrichment by small amounts of melt has been advocated (e.g. Crawford et al, 1989; Umino and Kushiro, 1989; Van der Laan et al., 1989; Defant and Drummond, 1990; Pearce et al., 1992a). Tracking fluid and melt components in the source of boninites reveals a diversity in the melt-forming processes that crucially constrain the evolution of mantle wedges in nascent volcanic arcs.

In New Caledonia, the clinoenstatite boninite of Nepoui has been previously described in detail by Sameshima et al. (1983), Cameron (1989), Black et al. (1994), Ohnenstetter and Brown (1992) and Solovova et al. (2012). Some authors considered the Nepoui boninite as part of the Late Cretaceous-Paleocene Poya Terrane and accordingly interpreted it as a product of back-arc magmatism (Eissen et al 1998; Crawford et al., 2003). Alternatively, other interpretations placed it in the post-obduction period (Black et al, 1994). Therefore, there is to date no agreement on the age and origin of these rocks. This article presents a synthesis of already published data combined with new geochemical (whole-rock and Nd-Sr) and geochronological data ($^{40}Ar/^{39}Ar$ and U-Pb ages). These comprehensive data sets allow a new interpretation to be forwarded.

Geological setting

New Caledonia corresponds to the emerged northern part of an elongated submarine ridge, the Norfolk Ridge, which is connected southward to the large continental plateau that also bears New Zealand. This continental fragment has been detached from Australia mainland in Late Cretaceous time at the end of Gondwana breakoff. The main island of New Caledonia is a mosaic of volcanic, sedimentary and metamorphic terranes, which were assembled during two major tectonic episodes; an Early Cretaceous tectonic collage; and a Paleocene to Late Eocene subduction followed by obduction/collision. Both events included periods of high-pressure metamorphism in connection with plate convergence in subduction zones.As such, the geological evolution of New Caledonia comprised three main episodes:

i) The Gondwanian phase (Permian-Early Cretaceous) is marked by subduction along the Southeast Gondwana margin. At that time, proto-New Caledonia was located in a fore-arc region in which volcanic-arc detritus accumulated; whilst accretion and subduction of oceanic and terrigenous material formed an accretionnary complex metamorphosed into the blueschist facies.

ii) During the Late Cretaceous to Eocene, marginal rifting isolated New Caledonia, and after a short period of shallow water terrigenous sedimentation associated with minor volcanic activity, only pelagic sediments accumulated. A new northeast-dipping subduction appeared to the east of New Caledonia at the Paleocene-Eocene boundary, it generated the eclogite-blueschist complex of northern New Caledonia, consumed the eastern Australian Plate, and eventually ended with Late Eocene obduction, when the Norfolk Ridge blocked the subduction zone.

iii) Finally, during the post-Eocene phase, New Caledonia definitively emerged; this episode mainly corresponds to tropical weathering of exhumed rocks, prominent regolith development and minor tectonic events.

The Paleogene geology of New Caledonia is characterized by a Eocene high-pressure metamorphic belt, exposed in the northernmost part of the island, and two large allochthonous terranes, emplaced during the Eocene, referred to as the Poya Terrane and the Peridotite Nappe (Fig 1).

The HP-LT belt comprised mafic blueschist and eclogite facies rocks and minor metasediments, crosscut by retrograde greenschist facies shear zones (albite schists). All these rocks recrystallised in a northeast-dipping subduction zone and now form a melange embedded in a metaserpentinite (talcschist) matrix (Cluzel et al., 2001). Maximum Pressures of ca. 24 kbar and temperatures of ca. 650°C are recorded by relict eclogite-facies assemblages (Clarke et al., 1997; Carson et al., 2000; Vitale-Brovarone and Agard, 2013). Peak metamorphic conditions have probably been reached during the Lower Eocene (ca. 44 Ma, U-Pb on metamorphic zircon overgrowths; Spandler et al., 2005). Mafic eclogites have Late Cretaceous to Eocene protolith ages and share geochemical affinities with the mafic Poya terrane (Cluzel et al., 2001; Spandler et al., 2005).

The lower allochthonous unit, termed Poya Terrane (or Nappe) (Cluzel et al, 1994, 1995), is an extensive mafic unit mainly exposed along the west coast of the island. The mafic Poya Terrane comprised sliced upper oceanic crust (basalt and dolerite), slightly metamorphosed (zeolite to lower greenschist facies) by ocean floor metamorphism. Variably colored (red, green, black) abyssal sediments appear in interpillows and upright lenses a few metres thick, which yield Campanian to Late Palaeocene radiolarians (c. 90-55 Ma; Aitchison et al, 1995; Cluzel et al, 2001). The Poya Terrane rocks are dominantly enriched MORB (E-MORB, ~80 %) with minor back-arc (BABB) and alkaline intraplate basalts (OIB), and cannot be genetically related to either enstatite-bearing gabbro cumulates, or ultra-depleted harzburgites of the Peridotite Nappe (Prinzhofer, 1987). Some Poya Terrane basalts display the geochemical features of oceanic plateaus and had been interpreted as such (Cluzel et al, 1997). However, their constant association with bathyal argillite suggests eruption at depth not less than 3,000 m and they cannot have formed a massive plateau such as Ontong Java (Kroenke, 1972). The Poya Terrane resulted from off-scrapping and slicing of lower plate crust in front of the intra-oceanic Loyalty Arc (Cluzel et al, 2001), forming a cordilleran-type ophiolite (Wakabayashi and Dilek 2003, Cluzel et al, 2012b). This mafic complex was thrust over autochthonous rocks of the Norfolk Ridge during the Late Eocene as recorded by syntectonic sedimentation (Maurizot and Cluzel, 2014). The Poya Terrane was in turn overthrust by the Peridotite Nappe in latest Eocene time (Cluzel et al., 1998).

The Peridotite Nappe (Avias, 1967), one of the World's largest ultramafic allochthons, originally covered most of the island. However, several phases of erosion left tectonic klippes spread along the west coast and a larger unit called "Massif du Sud" in the south of the island. Serpentinised peridotites (up to 100% serp.) exist at all levels of the Peridotite Nappe, independently of their distance to the base and may be related to several pre-obduction serpentinisation events (off ridge axis, fore-arc, …). Partly serpentinised peridotites are affected over more than 200-500m from the basal thrust by upward decreasing cataclasis, which is clearly related to obduction. Kinematic indicators in the highly sheared serpentinite sole, 0-200 m thick, generally indicate top to the southwest thrusting.

The Peridotite Nappe is dominantly composed of harzburgite (>80%), dunite and minor lherzolite (in northernmost massifs only) that represent a prominently depleted supra-subduction mantle lithosphere (Prinzhofer, 1981). Owing to their depletion in incompatible elements compared to primitive mantle composition, residual harzburgites underwent over 20-30% partial melting (Prinzhofer and Allègre, 1985; Marchesi et al., 2009), possibly followed by post-melting diffusion of incompatible elements that may account for extreme depletion (Prinzhofer, 1987; Pirard et al., 2013). They are overlain by dunite, pyroxenite, wehrlite and gabbro cumulates (Prinzhofer, 1987). Cumulate wehrlite and orthopyroxene-gabbro probably crystallized in equilibrium with boninite-series ultra-depleted melts (Marchesi et al., 2009; Pirard et al, 2013). These have almost certainly been eroded and are not preserved in the present geological record on the island. Whole rock and mineral chemical constraints allow a complex evolution to be drawn, from re-enrichment by circulating melts during oceanic accretion to mantle metasomatism during subduction (Marchesi et al., 2009; Ulrich et al., 2010; Spandler and Pirard, 2013; Secchiari et al., submitted). The timing of the inception of intra-oceanic subduction that eventually led to obduction, is constrained by high-temperature amphibolites of the metamorphic sole, dated at 56 Ma ($^{40}Ar/^{39}Ar$; Cluzel et al., 2012a).

The Peridotite Nappe is crosscut by a series of dikes emplaced at ca. 55-50 Ma (Early Eocene; Cluzel et al., 2006), which are not present in the Poya Terrane. These dikes comprise minor basalt (dolerite) and a variety of medium to coarse grain rocks, the compositions of which vary from ultramafic (pyroxenite and hornblendite) to felsic (diorite, leucodiorite and granite). Basalt dikes display supra-subduction affinities (island arc tholeiites), and likely represent the product of partial melting of “normal” mantle wedge. In contrast, the majority of felsic dikes are interpreted to be slab melts formed by partial melting of diverse oceanic mafic rocks including gabbro cumulates. Some of the felsic dykes have geochemical affinity with boninites and have been referred to as “boninite-series” (Cluzel et al., 2006). These “boninite-series” dikes will be compared with CE-boninite to address a possible common origin and provide additional constraints on the timing of boninite magmatism.

A simplified view of the geometrical relationships of autochthonous rocks, Poya Terrane, metamorphic sole, and Peridotite Nappe is presented on Fig. 2

The only known occurrences of clinoenstatite-bearing boninite in New Caledonia are located 10-13.5 km to the NW of village of Nepoui (Fig 1). In the main outcrop in a small quarry of the Plaine des Gaïacs (Fig 3 & 4a), boninite crops out in lenses or brittle boudins, a few metres thick, at the base of Peridotite Nappe, within the serpentinite sole. Boninite is generally massive and displays vitrophyric, locally vesicular texture. Angular (pillow ?) breccia is occasionally found (Fig 4b). Devitrification nodules 0.5-2 cm in diameter, occur sporadically and are generally altered into smectite. Cameron et al. (1983) have reported boninite floats on the upper slopes of Riviere Rouge watershed and in alluvium of this river near RT1 (main road). A well-crystallized and coarser grained boninite (dike ?) is overthrust by serpentinite on the bank of RT1 a few tens metres to the northwest of Rivière Blanche bridge, and sub-rounded clasts of boninite are present in alluvium of the same river (Sameshima et al., 1983; Cameron, 1989) (Fig 3). The floats and some outcrops are generally slightly weathered and appear as rounded boulders with onion-peel structure. However, fresh dark-colored glassy boninite blocks have been found in the quarry of Plaine des Gaïacs (164.911°E; 21.237°S).

These outcrops have been given a considerable attention in spite of their small size, and have been diversely interpreted as: i) post-45 Ma dike, lava flows and pillow-lavas (Cameron et al., 1983); ii) lava flows, pillow-lavas and dike of unknown age (Ohnenstetter and Brown, 1992; Solovova et al., 2012); iii) Miocene (i.e. post-obduction) intrusive rocks (Black et al., 1994); iv) rocks forming an integral part of a Late Cretaceous-Paleocene unit named West Coast Basalts (now renamed Poya Terrane) (Paris, 1981; Sameshima et al., 1983; Ulrich et al., 2010); v) rocks tectonically picked up during peridotite obduction (Eissen et al., 1998; Crawford et al., 2003).

However, the geological setting of the Poya Terrane and Peridotite Nappe rule out some of the previous interpretations. There are no lenses or slivers of Poya Terrane rocks within the serpentinite sole of the ophiolites in New Caledonia, and no boninite have been observed within the Poya Terrane. In addition, there are no clasts of boninite in the Eocene turbidites that record overthrusting of the Poya Terrane (Cluzel et al, 2001; Maurizot and Cluzel, 2014). Therefore, a direct connection of the Nepoui Boninite with the dominantly tholeiitic Poya Terrane is not supported by field, geochemical or isotopic evidence (Cameron, 1989). The porphyroclastic serpentine mylonite that surrounds the boninite also contains decimetre to metre-size sub-rounded boulders of diorite and leucodiorite, which have similar characteristics to the Early Eocene dike system that crosscuts the Peridotite Nappe, some of which with boninitic affinities (Cluzel et al, 2012a; this study).

For these reasons we follow Cameron’s conclusions (except for the age) and interpret Nepoui boninite as dike and lava flows, tectonically enclosed in the serpentinite sole of the ophiolite. These rocks together with the Early Eocene dikes that cross-cut the Peridotite Nappe, belong to the upper plate of the subduction/obduction system; in contrast, Poya Terrane rocks are derived from the lower plate (Cluzel et al, 2001). Due to the lack of stratigraphic contacts, the timing of boninite emplacement cannot be constrained by field evidence.

Mineralogical and geochemical features of Nepoui boninite have already been described in detail by previous authors (Sameshima et al., 1983; Cameron et al., 1983; Cameron, 1989;

Ohnenstetter and Brown, 1992; Solovova et al., 2012) and are only briefly outlined in this article. The Népoui boninite displays hyaloporphyritic texture with some 50-60% dark glassy groundmass enclosing poly-synthetically twinned clinoenstatite, orthopyroxene (bronzite) and olivine microphenocrysts, and accessory clinopyroxene, hornblende and chrome-spinel (chromite). Clinoenstatite laths 1-4 mm long, contain minute chromite grains and appear as decussate aggregates (Fig 5a & 5b).

The mineralogy, the high compatible elements and the very low TiO_2-K_2O contents, make the CE-boninite of Nepoui similar to other low-Ca boninites worldwide (Crawford et al., 1989). These have been interpreted to result from high temperature hydrous melting of a depleted peridotite (e.g., Cameron, 1989; Ohnenstetter and Brown, 1992; Eissen et al., 1998). Considering the high content in compatible elements, this interpretation can reasonably be maintained; however, it fails to explain the prominent LILE (large ion lithophile elements) contents.

Dating of boninitic magmatism

^{40}Ar/^{39}Ar dating results on Nepoui CE-boninite

Two samples (PLGA2 and PLGA3) of glassy clinoenstatite boninite from the Plaine des Gaïacs quarry have been selected, carefully avoiding devitrified zones. Both samples yielded well behaved ^{40}Ar/^{39}Ar age spectra and define two plateaus, each including 100% of the ^{39}Ar total gas release. PLGA2 gave an age of 47.4 ± 0.9 Ma (2σ; MSWD = 1.1; P =0.38) whereas sample PLGA3 yielded a slightly older age of 50.4 ± 1.3 Ma (MSWD = 0.70; P = 0.75) (Fig 6). Both samples show identical K/Ca spectra with a bimodal distribution of compositions and with values ranging from 0.15 for low temperature steps to 0.02 for high temperature steps. The invariance of the age of each individual step over such a variable K/Ca composition demonstrates that the samples did not contain secondary minerals. No inverse isochron age could be calculated due the cluster of the data near the $^{40}Ar^*/^{39}Ar_K$ radiogenic axis.

U-Pb on zircon dating of boninite-series dikes

Four representative samples, three leucodiorites and one granite, have been selected for U-Pb zircon dating among 10 boninite-series rocks sampled from various parts of the Peridotite Nappe in New Caledonia (for sample locations in the WGS 84 reference grid, see Table 4, online appendix). All dated samples have yielded ages that are within error of each other. All four samples cluster at 53.7±0.7 Ma (Fig. 7). No inherited cores have been noted in the analysed zircons (Fig. 8) and preclude any contamination by continental crust-derived melts.

Geochemistry, major and trace elements

Geochemistry of Nepoui CE-boninite

In total, eleven new analyses have been included in this study. Four boninite samples from the quarry of Plaine des Gaïacs, (two of them having also been used for dating purpose), one sample from a boulder in the Riviere Rouge (river; Fig 3), and four samples from the unpublished data of M.A. Audet's PhD (2008) (Table 2, online appendix). These new analyses are compared and discussed with that from the previously published data sets (Cameron, 1989; Sovolova et al., 2012).

Nepoui boninites have andesitic major elements contents (SiO_2 = 55.5 wt%, Al_2O_3 = 10.0 wt% on av. for 10 samples). They have low CaO (3.8 wt% on av.) and FeO contents (7.6 wt%) and characteristically have low CaO/Al_2O_3 (0.4 wt% on av.), very low K_2O (0.6 wt%) and TiO_2 (0.2 wt%); in contrast, they display high compatible elements contents (MgO= 11-15 wt%, Cr= 486-1371ppm, Ni= 190-1640 ppm) (Table 1, online appendix).

The abundance of crystals (see Figure 5) as well as the major and trace element variations (low CaO, high Cr and Ni) in most of the lavas are consistent with an origin by crystal accumulation. The lavas with the highest CaO concentrations (RRG1 and 2917) also have the lowest Cr and Ni values, and could most closely represent a liquid composition.

The Nepoui boninites generally display high whole-rock water contents (1.8-7.6 wt%H_2O) and 6-8 wt %H_2O in groundmass glasses (Solovova et al, 2012); in contrast, melt inclusions only contain up to 4 wt% H_2O. A significantly different H_2O content in groundmass and inclusions without formation of secondary minerals may record either seawater-melt interaction (Solovova et al, 2012); or alternatively, melt rehydration by magmatic waters coming from already crystallised rock.

The compositions of Nepoui boninite very closely resemble the average boninite of the Bonin Islands (Crawford et al., 1989) and Cape Vogel (König et al., 2010). Slightly concave "spoon-shaped" REE patterns of most boninite samples do not significantly differ from one sample to another. However, one of the samples reported by M.A. Audet (2008; #2915) displays bulk LREE enrichment with a negative Ce anomaly (dotted pattern on Fig 8a). REE enrichment may be due to downward input of supergene REE from the weathering profile of peridotites where Ce^{4+} accumulates with Fe oxide (Braun et al., 1990) and this sample will not be considered further. Nepoui boninites are REE-rich (10 to 20 times the chondrite), and display significant LREE enrichment ($(La/Sm)_n$= 2.2). Compared with the data of literature, the REE patterns of Nepoui boninites very much resemble that of Cape Vogel (König et al, 2010) with higher average bulk REE content though (Fig 8a).

On the expanded REE and trace elements spiderdiagram (Fig 9a), Nepoui and Cape Vogel boninites display similar patterns, although Nepoui rocks are richer in incompatible elements and at first sight seem less depleted in HREE and HFSE. LILE vs. HFSE fractionation may be due to source mineralogy (HFSE-retaining refractory minerals); or alternatively, due to enhanced LILE and bulk REE enrichment; these alternative interpretations will be discussed below. Nepoui and Cape Vogel boninites both display a well-defined negative anomaly in Nb and Ta and a positive anomaly in Zr and Hf (Fig 9a) and most probably have been generated in a similar way.

Geochemistry, major and trace elements of boninite-series dikes

Some dikes that crosscut the Peridotite Nappe, which are generally referred in the field to as leucodiorites or diorites depending on their amphibole content, are to some extent geochemically similar to CE-boninites. The dikes are generally a few cm to a few metres thick and extend over several metres or tens metres. They are dominantly coarse grained felsic rocks with minor ferromagnesian minerals (orthopyroxene, hornblende, biotite), and develop reaction rims (anthophyllite) against the peridotite wall rock. Some others with similar compositions and textures are metre-scale porphyroclasts or brittle boudins enclosed in the serpentinite-mylonite sole of the Peridotite Nappe. In spite of some scatter, dike orientations cluster around ENE-WSW and WNW-ESE directions. Boninite-series dikes cannot be distinguished in the field from the other types of felsic intrusive rocks and a geochemical discrimination is necessary. On the basis of their total alkali and silica contents, they may be referred to as syenites and syeno-diorites. On the TAS diagram (Le Bas, 1986, not represented), they do not form one single differentiation trend with CE-boninites due to their higher alkali content. In general the incompatible elements contents are 1 to 10 times greater than that of CE boninite, consistent with the higher alkali contents. They display “spoon-shaped” REE patterns similar to that of CE-boninite with higher REE contents though (Fig 8b). Positive and negative Eu anomalies irrespective of the bulk REE or SiO_2 contents may be an effect of plagioclase fractionation; or alternatively, result from a source feature (Cluzel et al, 2006). On the expanded REE and trace elements spiderdiagram, the patterns of boninite-series rocks display the same negative anomalies in Nb and Ta, and positive anomalies in Zr and Hf (Fig 9b). Elemental ratios Nb/Ta and Zr/Hf (with some exceptions probably due to Hf analytical issues) are consistent with that of CE-boninites. The comparison between the

Nepoui boninites and the boninite-series dikes shows that although they have small differences in chemistry and ages they also have strong geochemical similarities reinforcing the links between the two Early Eocene magmatic events .

Sr and Nd isotope geochemistry

The already published Sr and Nd isotope data on Nepoui boninite reported high Nd isotope range of values compared to other boninite localities (Cameron et al, 1983; Cameron, 1989). To check this feature, two new CE-boninite samples have been analyzed at the CNRS isotope laboratory of Clermont-Ferrand (France).

The two new CE-boninite samples provided $\varepsilon_{Nd(50)}$ of +7.9 , and $(^{87}Sr/^{86}Sr)_i$ of 0.704232 (±7) and 0.702359 (±5) respectively (Table 2, online appendix; Fig 10). These Nd ratios are within the range of moderately depleted mantle sources and strikingly differ from that of the nearby E-MORB basalts of the Poya Terrane ($+3<\varepsilon_{Nd(80)}<+6$; Cluzel et al., 2001), In contrast, Nd isotopic ratios are similar to that of BABB of the Poya Terrane ($+7<\varepsilon_{Nd(80)}<+8.3$; Cluzel et al., 2001). It is worth noting that the isotopic signature of Nepoui CE-boninite also differs from that of Cape Vogel, which display “enriched” signatures in spite of some compositional (REE and trace elements) similarity. Only one Nd-Sr isotope analysis of a boninite-series dike is available. The leucodiorite MeM2 provided $\varepsilon_{Nd(54)}$ of +8.7, and $(^{87}Sr/^{86}Sr)_i$ of 0.702782 (±7) (Table 2; Fig 10). This data confirms that although the CE-boninite and boninite-series felsic dikes are not genetically related by a simple differentiation process the two suites have been similarly generated by moderately depleted mantle sources.

Source of Nepoui CE-boninite ; the role of additional components.

The partial melting of a depleted peridotite alone cannot account for the geochemical and isotopic features of Nepoui CE-boninite. LREE- and more generally, LILE enrichment is a common feature of boninites, which has been explained by invoking source re-enrichment by either an OIB-type component (Macpherson and Hall, 2001) or, a subduction component (fluid and/or melt) (Hickey and Frey, 1982; Tiepolo et al., 2000, 2002; König et al., 2010; Spandler and Pirard, 2013). Involvement of a subduction component is also suggested by prominent Zr and Hf positive anomaly (Kamenetsky et al., 2002; König et al., 2010) (Fig 9a).

Discrimination between fluid and melt enrichment has been attempted using Ba/Th-Th diagram (König et al., 2010) (Fig 11). Compared to MORB composition (Sun and McDonough (1989), relatively high Ba/Th ratios (150-300) suggest the role of a subduction-derived fluid for some Nepoui boninite samples; however most of them bear the signature of a melt-enriched source (Ba/Th < 100; Th= 0.2- 0.7 ppm), very similar to that of Cape Vogel boninites (Fig 11).

In order to better constrain the possible source of a slab melt component, the approach developed by König et al. (2010) for the Cape Vogel boninites has been undertaken on Nepoui boninite. Melting metamorphic rocks generates fractionation of some element ratios, which depend upon source mineralogy (e.g. metamorphic grade in a subduction zone) because residual minerals strongly control the budget of some trace elements. Assuming that the source rock had a MORB composition, it may be suggested that similarly to Cape Vogel boninite, shift toward higher Zr/Sm ratios (Fig 12) and lower Nb/Ta (Fig 12a) and Nb/La (Fig 12b) denotes the presence of residual amphibole in the solidus. In contrast, the increase of Zr/Sm compared to MORB compositions suggests that rutile was not present in the source as a refractory phase (König et al, 2010). Strong positive anomalies in Zr and Hf (Fig. 9b) suggest that zircon was not residual in the source of CE-boninites and could not account for the Zr/Sm ratio. The occurrence of a small amount of residual garnet is also suggested by some HREE fractionation ($1.1<Gd_n/Yb_n<1.4$; Fig 12c) (Tiepolo et al., 2000; Foley et al., 2000, 2002). Therefore, Nepoui boninites bear the signature of MORB-derived slab melts, which were likely formed by partial melting of rutile-free, garnet-amphibole bearing mafic rock. It is worth noting that BABB-like barroisitic eclogites of the Eocene metamorphic complex of northern New Caledonia and high-grade BABB-like HT amphibolites of the metamorphic sole share some of the geochemical and isotopic signatures of Eocene dikes ($7.1 < \varepsilon_{Nd} < 8.3$; Cluzel et al., 2001; 2012), and thus are possible candidates for slab melt sources. This assumption will be used in the modeling presented below.

Genesis of Nepoui CE-boninite ; a modeling approach.

Melting models used in oceanic-ridge settings are unable to account for the complex processes that occur in supra-subduction zones, particularly because some parameters, e.g. partition coefficients are highly sensitive to fluid circulations and/or temperature variations. In order to establish the processes responsible for CE-boninite genesis, a model has been developed, which shows that CE-boninites have been likely generated from a three-step evolution. This evolution includes: (i) initial melt extraction and peridotite depletion in a ridge setting; (ii) partial slab melting in a subduction zone and mantle wedge re-enrichment by slab melts; and (iii) hydrous melting of the re-enriched mantle wedge (Fig. 14). All parameters used in this model are listed in Table 3 (online appendix).

It is well established that boninites come from the melting of a highly refractory mantle source that has previously experienced melt extraction. The first step of melt extraction may have occurred in a mid-ocean ridge (e.g. Cameron, 1983; Crawford et al., 1989; Arndt, 2003; König, 2010); or more likely, a marginal basin, which would account for the geodynamic setting of the basins that opened during the Late Mesozoic break-off of the SE-Gondwana margin. The first melting stage is assumed to generate a depleted mantle. Melt and residue compositions have been computed using a model of anhydrous non-modal fractional melting (Shaw, 1970; McDade et al., 2003a) of a primitive mantle source (McDonough and Sun, 1995; Robinson et al., 1978) (Fig. 14a). The resulting residue represents the assumed composition of pre-subduction mantle wedge (Table 4, online appendix).

The second step aims at modeling the trace element composition of the slab melts that have been formed during or shortly after subduction inception. The subduction that eventually gave birth to obduction in New Caledonia started at (or near) the ridge of the South Loyalty (or East New Caledonia) Basin (SLB) at ~56Ma (Cluzel et al, 2012a). At subduction inception, when the spreading center changed into a subduction zone, the thermal gradient was as high as 40°/km, and generated the high-temperature amphibolites of the metamorphic sole (Cluzel et al, 2012); thus, at the time of boninite genesis (~50-47Ma; this article) the tip of the subducted slab was 6-9My-old, and still hot. Therefore, the PTt path of a slab of about the same age (Thorkelson and Breitsprecher, 2004) has been used in the model (Fig. 13). On the basis of this PTt path and the wet basalt solidus of Harry and Green (1999), slab rocks are unlikely to melt above 65 km depth (~2 GPa). At a pressure of 2.0 GPa, a rock of basalt composition is metamorphosed into eclogite, thus providing constraints on source mineralogy. In addition, some element ratios in Nepoui CE-boninite indicate a significant influence of slab melts derived from an amphibole-bearing source (see “role of additional components” section above). Therefore, to account for the composition of resulting rocks, the average chemical composition of BABB-like eclogites of Northern New Caledonia (Cluzel et al., 2001; Spandler et al, 2005) has been used to represent the source of slab melts (Fig. 14c). Considering these rocks as a melt source makes sense because (i) they have recrystallized in the same Eocene (Spandler et al, 2005) subduction zone, (ii) they yield isotopic ratios consistent with Nepoui boninite (in contrast with E-MORB-like eclogite of the same terrane; Cluzel et al, 2001), and (iii) they contain a significant amount of amphibole (barroisite; Clarke et al, 1997). Considering the PTt path of a 5 Ma-old slab and the stability field of hornblende, slab melting is likely to occur in a small PT window, as illustrated in Figure 13. Slab melting has been modeled using 6 % batch melting of BABB-like eclogite computed with temperature-dependent hydrous partition coefficients of Kessel et al. (2005) using temperature-dependent relationship from Kimura et al. (2009, 2010) at 820°C (temperature at the slab surface). Modeling results in a felsic melt composition (Fig 14b), which is strikingly similar to that of some slightly older dikes (55-50 Ma U-Pb on zircon) that cross-cut the ophiolite (Cluzel et al, 2006). It is worth noting that a sediment contribution has not been considered because the young age of the oceanic crust and intra-oceanic character of the subduction most probably prevented significant amounts of bathyal sediments to be involved. The low $^{87}Sr/^{86}Sr$ ratio of Nepoui boninite is consistent with this assumption.

The formation of boninites occurred during a third stage that involved a fore-arc, refractory mantle wedge (i.e. the residual pre-subduction mantle formed during the first stage) contaminated by the slab-derived melts. The melting process is modeled using a non-modal batch melting model (Shaw, 1970) (Fig. 14c). The mineral mode is from McDade et al. (2003b), and partition coefficients are after Kessel et al. (2005), using temperature-dependent relationship from Kimura et al. (2009). The best-fit results suggest that the melting ratio of the supra-subduction mantle was 25% at a temperature of 1350°C, with a slab-melt contribution to the boninite source of ~3%. These results are consistent with that of literature (Crawford et al., 1989; Pearce et al., 1992b; Sobolev and Danyushevsky, 1994; Arndt, 2003; Leng et al., 2012; Li et al, 2013).

Testing a possible genetic link between CE-boninite magma, gabbro cumulates and refractory harzburgite of the Peridotite Nappe.

Several cumulate “lenses”, a few km wide, occur in the Massif du Sud (Ouen Is; Prony Bay; Mouirange and Montagne des Sources) (Fig 1), all have ultramafic rocks at the base and gabbros on top. Extremely depleted orthopyroxene gabbros are thought to have crystallized from boninite magma in a fore-arc setting (Marchesi et al, 2009; Pirard et al, 2013), but the corresponding boninitic crust if any, has been eroded out, thus preventing any check of this hypothesis. Considering the age of Nepoui boninite situated between subduction inception and final obduction, a genetic link should be searched between boninite magma injected along/across the subduction zone and those who possibly erupted in the fore-arc. This hypothesis has been tested by applying a fractional crystallization process to the modeled boninite from Figure 14c (Table 4, online appendix). Using the average mineral modes given in Marchesi et al. (2009), it appears that gabbroic cumulates may derive from 30% fractional crystallization of a magma compositionally similar to Nepoui CE-boninite (Fig 14d).

A possible genetic link between boninites and the highly refractory harzburgite, which underlie cumulate gabbros has been already postulated (e.g. Eissen et al, 1998; Crawford et al., 2003; Ulrich et al. 2010; Pirard, 2013). This hypothesis has also been tested by comparing the modeled residue of boninite production with new accurate geochemical data on NC harzburgite (Secchiari A., work in progress). The residual mantle composition calculated after boninite extraction is shown on Figure 15 (Table 4, online appendix). Although the modeled result shares some features with NC harzburgites, i.e. general outline of trace element patterns, U, Pb, Sr, Zr and Hf positive anomalies, it fails to reproduce the extreme depletion that characterizes these rocks. Therefore, it appears that New Caledonia's harzburgites were not formed as a direct consequence of CE-boninite melt extraction. Instead, they may result from a more complex polyphase evolution involving several melting events followed by fluids and/or melts circulations.

Timing of Nepoui CE-boninite emplacement

The two Nepoui boninite samples yielded plateau ages at 50.4 ± 1.3 Ma and 47.4 ± 0.9 Ma. The robust age spectra show no sign of perturbation and therefore, may be interpreted as emplacement ages. The two ages are very close, but not indistinguishable at the 2σ level; however, the apparently younger sample yields slightly higher LOI (5.2 vs. 4.4 wt%). Late-magmatic rehydration inferred from the comparison of crystal and glass phases (Solovova et al., 2012) and variable ($^{87}Sr/^{86}Sr)_i$ as well, may also induce some elemental mobility and hence, apparent age discrepancy. The similarity with some "boninite-series" Early Eocene dikes suggest that they have been emplaced during two magmatic episodes that are very close in terms of timing and tectonic setting.

As a consequence, Nepoui CE-boninite can no longer be considered as a post-obduction dike; or part of the Poya Terrane, which has been shown to be older than 55 Ma, and obviously comes from different mantle and slab sources (Cluzel et al., 2001). Alternatively, $^{40}Ar/^{39}Ar$ apparent ages at 47-50 Ma and some geochemical similitude allow it to be chronologically and partly genetically correlated with the Early Eocene dike complex of the Peridotite Nappe although it seems to be slightly younger. Considering the age of Nepoui boninite situated between subduction inception and final obduction, a genetic link between CE-boninite found in the serpentinite sole and those erupted in the fore-arc and formed enstatite gabbro cumulates is most likely.

Source of Nepoui CE-boninites

As most boninites, Nepoui rocks have been formed by hydrous partial melting of a depleted peridotite re-enriched by additional components that may account for LILE contents of the resulting melt. It is worth noting that in the case of ultramafic source re-enriched by melts, the bulk of trace elements Rb, Sr, Nd and Sm come from the additional component. As a consequence, the isotopic signature is strongly (not to say dominantly) influenced by the source of additional melts; therefore, isotope ratios are good tracers of metasomatic material.

ε_{Nd} values for Nepoui boninites (+7.9), which are in the range of "moderately depleted MORB sources", contrast with the undepleted Cape Vogel boninites ($3.9 < \varepsilon_{Nd} < 5.2$) (Fig 10), and question the involvement of an asthenospheric component (OIB-like, or E-MORB-like), which would result in lower values of ε_{Nd}. Alternatively, source contamination by slab melts derived from BABB-like crust would result in such isotopic signature.

Nd isotopic ratios of Nepoui boninite ($\varepsilon_{Nd(50)}$=7.9) are in the same range of values than that of Early Eocene dikes (8.7<$\varepsilon_{Nd(53)}$ <6.0; 7.5 on average; Fig. 10) (Cluzel unpubl. data). Therefore, the component that re-enriched the peridotite source is most probably a small amount of melt formed by partial melting of subducted oceanic crust; thus resulting in moderately depleted MORB-like isotopic signature. This added component shares most of the geochemical and isotopic features of Early Eocene felsic dikes, which at least partly come from partial melting of the lower plate of the subduction system; e.g., high-temperature amphibolite or eclogite-facies rocks.

Pacific-scale correlations

There is some age similarity between boninites from New Caledonia and those of the Izu-Bonin-Mariana arc (IBM; ca 51-52 Ma; Ishizuka et al. 2006, 2011; Reagan et al., 2008, 2013) and a long distance correlation is tantalizing. Such correlation has already been proposed between IBM and Tonga-Kermadec (TK) arcs because fore-arc magmatism started at about the same time (Stern et al, 2012). Recently, a further correlation has been made possible by the discovery of Eocene inherited zircons in Western Vanuatu Arc volcanics (Buys et al, 2014), a part of the Vitiaz Arc rifted at ca 10Ma. This discovery confirms the existence of a continuous Eocene west-dipping subduction in the western Pacific (Fig 16). Synchronous subduction inception over such a distance suggests one single Pacific-scale event, which could involve New Caledonia as well. However, subduction inception in New Caledonia is constrained by the age of the metamorphic sole of the ophiolite, which recrystallised at ca. 57 Ma, e.g. 4-5My before IBM-TK, with an opposite polarity (Fig 16). In addition, fore-arc magmatism of the IBM arc includes thick basalt series underlying the boninites, which are absent in New Caledonia. Therefore, a different mechanism of subduction inception should be advocated and correlation of Eocene events in New Caledonia at a regional scale probably needs some additional exploration.

Conclusion

Owing to its overall features, Nepoui CE boninite may be interpreted as volcanic rocks and shallow dikes emplaced during the Early Eocene. Boninite magma possibly circulated along the serpentinised hanging wall of the subduction zone that eventually formed the tectonic sole of Peridotite Nappe. REE and other trace elements contents, source modeling and isotopic signatures as well suggest that the depleted peridotite source was re-enriched by felsic melts formed by partial slab melting during the early stage of intra-oceanic subduction at 55-50 Ma (Fig 17a & b). Water influx into the mantle wedge due to subduction of slightly older (cooler and hydrated) lithosphere was responsible for low degree partial melting of the re-enriched mantle wedge, and generated boninitic magma (Fig 17c). It is suggested that enstatite-bearing gabbro cumulates formed the base of a (discontinuous?) fore-arc crust dominantly formed of CE-boninite; whilst only minor amounts of CE-boninite magma were injected along the subduction zone. Thereafter, the fore-arc was frozen and a “normal” mantle wedge established that generated the yet poorly investigated Loyalty Arc (Fig 17d). Finally, the northern tip of the Norfolk Ridge reached the subduction zone and blocked it. As a result, two successive obductions occurred during the Late Eocene (mafic Poya Terrane), and latest Eocene (ultramafic Peridotite Nappe) respectively (Fig 17e). During the latter event, CE-boninite lenses were pinched and wrapped in serpentinite-mylonite near the base of the ultramafic allochthon. Meanwhile, the bulk of the uplifted fore-arc boninitic crust was eroded out and only leaved cumulate remnants. Considering the bulk evolution of the Southwest Pacific during the Late Cretaceous-Eocene period, it may be suggested that the upper mantle rocks that now form the Peridotite Nappe have been inherited from a first phase of marginal (back-arc?) basin opening during the Late Cretaceous Gondwana breakoff. These older and already depleted peridotites; again evolved in a fore-arc setting and were metasomatised by slab-related fluids and melts during the Eocene subduction.

Acknowledgements

This work has been partly funded by a special grant of the Scientific Council of the University of New Caledonia. C. Mayer and Z. Martelli (Curtin University) are thanked for her help with the sample preparation for $^{40}Ar/^{39}Ar$ dating, and T. Holmes (UTAS) for heavy mineral separation. DC acknowledges Pr. Anthony J. Crawford to whom he wins a bet about the age of Nepoui boninite, for stimulating discussions years ago about amazing rocks of New Caledonia. Dr. J.A. Pearce and anonymous reviewers are warmly thanked for their constructive comments and suggestions.

Figure captions

Figure 1: Geological sketch map showing the location of Nepoui CE-boninite in the framework of mafic and ultramafic allochthons of New Caledonia.

Figure 2: Geological map of Plaine des Gaiacs area (Maurizot and Vendé-Leclerc, 2009) (see location on Fig. 1). The bold line locates the cross section Fig 3.

Figure 3: Sketch cross section (scale is only approximative) to show the geometrical relationship of autochthonous and allochthonous terranes of New Caledonia and location of CE-boninite and boninite-series dikes.

Figure 4: Outcrop features of Nepoui boninite. 4a: boninite boulder wrapped by serpentinite of the Plaine des Gaïacs quarry; 4b: vesicular boninite breccia (same location).

Figure 5: Texture of Nepoui boninite. 5a, sample of hyaloporphyritic boninite showing decussate aggregates of clinoenstatite. 5b, Microphotograph to show the micro-porphyritic texture.

Figure 6: $^{40}Ar/^{39}Ar$ step heating ages and K/Ca spectra of boninite glasses extracted from samples PLGA2 and PLGA3 (Plaine des Gaïacs quarry). All ages are given at 2σ and include all sources of uncertainties.

Figure 7: Reverse concordia diagram showing the U/Pb isotopic ratios of zircons for four representative samples of boninite-series felsic dikes. The majority of the data is concordant clustering at 54 Ma. Solid line entitled “common Pb” and 54 Ma isochron (calculated by the isoplot program of Ludwig 2003) are anchored to single stage Pb at 54 Ma (Stacey and Kramer, 1978).

Figure 8a & b: Chondrite-normalised REE patterns after Pearce (1982) (data from Table 1). 8a: the data of Early Eocene Nepoui boninite (plain lines) is from Cameron (1989), Audet (2008), Solovova et al. (2012; dark grey pattern), and this study. The dashed line pattern corresponds to the sample 2915*, probably REE-enriched by supergene fluids. Fields of boninites of Cape Vogel (light grey pattern) (König et al. (2010) and Bonin Islands (Ishizuka et al. 2006, 2011; striped pattern) are shown for comparison. 8b: REE patterns of boninite-series felsic dikes of the Peridotite Nappe. The dotted lines represent samples that have been dated by the U-Pb on zircon method. The normalisation value (C1) is from Evensen et al. (1978).

Figure 9a&b: Rare-earth and trace elements expanded spider diagram normalised to the primitive mantle (PM, after Hofmann, 1988). 8a: spiderdiagrams of Nepoui boninite, the dark grey area depicts the compositional field of boninites from Solovova et al. (2012), and the light grey pattern represents the field of compositions of Cape Vogel boninites. 9b: spiderdiagrams of boninite-series felsic dikes of the Peridotite Nappe. Data has the same provenance as Fig. 8 (Table 1).

Figure 10: $^{87}Sr/^{86}Sr$ versus $^{143}Nd/^{144}Nd$ plot of Nepoui boninite corrected for in situ decay at 50 Ma, and one boninite-series felsic dike (MeM2) corrected at 54Ma, compared to the fields of Cape Vogel boninites (grey pattern; König et al., 2010), Poya Terrane basalts (criss-crossed pattern; Cluzel et al., 2001), and Early Eocene dikes (stripped pattern; Cluzel et al., unpublished data). Shift toward higher values of $^{87}Sr/^{86}Sr$ probably denotes moderate elemental mobility in sample PO42 and in certain Early Eocene dikes. Bulk Solid Earth (BSE) and Depleted MORB Mantle (DMM) data are from Workman & Hart (2005).

Figure 11: Ba/Th versus Th plot of Nepoui boninites compared to Cape Vogel boninites. Data for N-MORB are from Arevalo & McDonough (2010); BABB from PETLAB data base (http://pet.gns.cri.nz/#/).

Figure 12: Plot of representative trace-element ratios used in discriminating the mineralogy of the source of slab melts (König et al, 2010)

Figure 13: Pressure–temperature and phase-stability diagram for 5 My-old subducted slab (Poli and Schmidt, 2002; Thorkelson and Breitsprecher, 2004, and references therein). The orange area indicates PT conditions where the young and hot South Loyalty Basin slab is expected to melt.

Figure 14: Results of CE-boninite modeling. A complete set of the parameters used in this model is given in Table 3. a) Primitive mantle-normalized trace element composition of the

residual mantle after MORB-type melt extraction, i.e. pre-subduction depleted mantle of the SLB. b) Trace element concentration of slab-derived melt resulting of the melting of the eclogitized SLB oceanic crust. The latter has been computed using the average chemical composition of BABB-like Eocene eclogites of Northern New Caledonia from Spandler et al. (2005). c) Trace element composition of NC boninites modeled as the result of the melting of pre-subduction depleted mantle (Fig 13) contaminated by slab derived melts (b). d) Fractional crystallization of modeled CE-boninites compared to enstatite gabbro cumulates of Montagne des Sources (Marchesi et al., 2009). Mineral modes used in this simulation are an average from Marchesi et al. (2009): Cpx: 41%, Opx: 13%, Plg: 42%, Ol: 4%. Best fit is obtained with F=30%. Partition coefficients for Cpx, Opx and Ol are from Kessel et al. (2005), using temperature-dependent relationship from Kimura et al. (2009) at T = 1000°C.

Figure 15: Comparison of the computed refractory residue (from the model Fig 14d) with NC harzburgite compositions (Secchiari A., PhD thesis in progress). The modeled residue is obviously much less depleted than the average harzburgite (Table 4) and allows ruling out a direct genetic relationship of the latter with gabbro cumulates.

Figure 16: West Pacific sketch map to show the continuous Eocene continent-ward dipping subduction zone that possibly extended from Japan to New Zealand, through Vitiaz and Tonga-Kermadec arcs; and in contrast, the Pacific-ward dipping subduction of New Caledonia and its possible extension to New Zealand (modified from Stern et al, 2012 and Cluzel et al, 2001).

Figure 17: Geodynamic model for boninite genesis in the framework of New Caledonia evolution during the Eocene (modified from Cluzel et al, 2012a).

References

Aitchison J.C., Meffre S. and Cluzel D. 1995. Cretaceous/Tertiary radiolarians from New Caledonia, Geol. Soc. of New Zealand Miscelaneous Publ. 81A, p. 70

Anderson R.N., Uyeda S., Miyashiro A., 1976. Geophysical and geochemical constraints at converging plate boundaries Part I: Dehydration in the downgoing slab, Geophys. J. Int. RAS 44, 333-357.

Arevalo R. Jr., and McDonough W. F., 2010. Chemical variations and regional diversity observed in MORB. Chemical Geology 271, 70–85. doi:10.1016/j.chemgeo.2009.12.013

Arndt, N. 2003. Komatiites, kimberlites, and boninites, J. Geophys. Res., 108, 2293, doi:10.1029/2002JB002157, B6.

Audet M.A., 2008. Le massif du Koniambo, Nouvelle-Calédonie: formation et obduction d'un complexe ophiolitique du type SSZ. Enrichissement en nickel, cobalt et scandium dans les profils résiduels. Unpubl. PhD thesis, University of New Caledonia, 327 p.

Baker, J., Peate, D., Waight, T. and Meyzen, C., 2004. Pb isotopic analysis of standards and samples using a Pb-207-Pb-204 double spike and thallium to correct for mass bias with a double-focusing MC-ICP-MS. Chemical Geology, 211, 275-303.

Bizimis M., Salters V.J.M., Bonatti E. 2000. Trace and REE content of clinopyroxenes from supra-subduction zone peridotites. Implications for melting and enrichment processes in island arcs. Chemical Geology 165, 67-85.

Black P.M., Itaya T., Ohira T., Smith I.E.M. and Tagaki M. 1994. Mid-Tertiary magmatic events in New Caledonia: K-Ar dating of boninite volcanism and granitoid intrusives. Geosci. Repts. Shizuoka University 20, 49-53.

Braun J.J., Pagel M., Muller J.P., Billong P., Michard A. and Guillet B. 1990. Cerium anomalies in lateritic profiles. Geochim. Cosmochim. Acta 54 (3), 781-795.

Buys J., Spandler C., Holm R. J., and Richards S.W., 2014. Remnants of ancient Australia in Vanuatu: Implications for crustal evolution in island arcs and tectonic development of the southwest Pacific. Geology 42, 939-942.

Cameron W.E. 1989. Contrasting boninite-tholeite associations from New Caledonia. In: A.J. Crawford ed., Boninites and related rocks, 314-338, Unwin Hyman, London.

Cameron W.E., McCulloch M.T. and Walker D.A. 1983. Boninite petrogenesis: chemical and Nd-Sr isotopic constraints. Earth Planet. Sci. Let. 65, 75-89.

Carignan J., Hild P., Mevelle G., Morel J. and Yeghicheyan D. 2001. Routine analyses of trace elements in geological samples using flow injection and low pressure on-line liquid chromatography coupled to ICP-MS: a study of geochemical reference materials BR, DR-N, UB-N, AN-G and GH. Geostandards Newsletter 25, 2-3, 187–198, DOI: 10.1111/j.1751-908X.2001.tb00595.x

Clarke G., Aitchison J.C., and Cluzel D. 1997. Eclogites and blueschists of the Pam Peninsula, NE New Caledonia : a reappraisal. Jour Metam. Petrology 38, 7, 843-876.

Cluzel D., Aitchison J.C., Clarke G., Meffre S. et Picard C. 1994. Point de vue sur l'évolution tectonique et géodynamique de la Nouvelle-Calédonie, C. R. Acad Sci. Paris. 319, 6, 683-688.

Cluzel D., Picard C., Aitchison J., Laporte C., Meffre S. et Parat F. (1997), La Nappe de Poya (ex-Formation des basaltes) de Nouvelle-Calédonie (Pacifique SW), un plateau océanique Campanien-Paléocène supérieur obducté à l'Eocène supérieur. C. R. Acad Sci. Paris. 324, 443-451.

Cluzel D., Chiron D. et Courme M.D., 1998. Discordance de l'Eocène supérieur et événements pré-obduction en Nouvelle-Calédonie (Pacifique sud-ouest) C. R. Acad Sci. Paris 327, 485-491.

Cluzel, D., Aitchison, J.C. Picard, C., 2001. Tectonic accretion and underplating of mafic terranes in the Late Eocene intraoceanic fore-arc of New Caledonia (Southwest Pacific): geodynamic implications. Tectonophysics 340, 23-59.

Cluzel D., Meffre S., Maurizot P., Crawford A.J., 2006. Earliest Eocene (53 Ma) convergence in the Southwest Pacific; evidence from pre-obduction dikes in the ophiolite of New Caledonia. Terra Nova 18, 395-402.

Cluzel D., Jourdan F., Meffre S., Maurizot P., and Lesimple S. 2012a. The metamorphic sole of New Caledonia ophiolite; $^{40}Ar/^{39}Ar$, U-Pb, and geochemical evidence for subduction inception at a spreading ridge. Tectonics. 31, 3, doi:10.1029/2011TC003085, 2012.

Cluzel D., Maurizot P., Collot J. and Sevin B. 2012b. An outline of the Geology of New Caledonia; from Permian-Mesozoic Southeast-Gondwanaland active margin to Tertiary obduction and supergene evolution. Episodes 35, 1, 72-86.

Crawford A.J., Falloon T.J. and Green D.H. 1989. Classification, petrogenesis and tectonic setting of boninites. In: A.J. Crawford ed., boninites and related rocks, 2-49, Unwin Hyman, London.

Crawford A.J., Meffre S., and Symonds P.A., 2003. 120 to 0 Ma tectonic evolution of the Southwest Pacific and analogous geological evolution of the 600 to 220 Ma Tasman Fold Belt System. Geological Society of Australia, Special Publication 22, 377-397.

Defant, M. J. and Drummond, M. S. 1990. Derivation of some modern arc magmas by melting of young subducted lithosphere. Nature 347, 662-665.

Eissen, J.P., Crawford, A.J., Cotten J., Meffre S., Bellon H., Delaune M., 1998. Geochemistry and tectonic significance of basalts in the Poya Terrane, New Caledonia. Tectonophysics, 284, 203-219.

Evensen N. M., Hamilton P. J. & O'Nions R. K. 1978. Rare earth abundance in chondritic meteorites. Geochimica et Cosmochimica Acta 42, 1199–212.

Foley S. F., Barth M. G. and Jenner G. A., 2000. Rutile/melt partition coefficients for trace elements and an assessment of the influence of rutile on the trace element characteristics of subduction zone magmas. Geochim. Cosmochim. Acta 64, 933–938.

Foley S.F., Tiepolo M. and Vannucci R., 2002. Growth of early continental crust controlled by melting of amphibolite in subduction zones. Nature 417, 837–840.

Halpin, J.A., Jensen, T., McGoldrick, P., Meffre, S., Berry, R.F., Everard, J.L., Calver, C.R., Thompson, J., Goemann, K., Whittaker, J.M. 2014. Authigenic monazite and detrital zircon dating from the Proterozoic Rocky Cape Group, Tasmania: Links to the Bel-Purcell Supergroup, North America. Precambrian Research.250, p.50-67.

Harry, D.L., Green, N.L., 1999. Slab dehydration and basalt petrogenesis in subduction systems involving very young oceanic lithosphere. Chemical Geology 160, 309-333.

Hickey R.L. and Frey F.A., 1982. Geochemical characteristics of boninite series volcanics: implications for their source. Geochimica et Cosmochimica Acta 46, 11, 2099–2115. doi: 10.1016/0016-7037(82)90188-0

Hofmann A.W., 1988. Chemical differentiation of the earth - The relationship between mantle, continental crust, and oceanic crust. Earth Planet. Sci. Lett. 90, 297-314.

Hyndman R.M. and Peacock S.M., 2003. Serpentinization of the forearc mantle. Earth Planet. Sci. Lett. 212, 417-432.

Ishizuka O., Kimura J.-Y., Li Y.B., Stern R.J., Reagan M.K., Taylor R.N., Ohara Y., Bloomer S.H., Ishii T., Hargrove U.S., Haraguchi S., 2006. Early stages in the evolution of Izu–Bonin arc volcanism: New age, chemical, and isotopic constraints. Earth Planet. Sci. Lett. 250, 385-401.

Ishizuka O., Tani K., Reagan M.K., Kanayama K., Umino S., Harigane Y., Sakamoto I., Miyajima Y., Yuasa M., Dunkley D.J., 2011. The timescales of subduction initiation and subsequent evolution of an oceanic island arc. Earth & Planetary Science Letters 306, 229-240.

Jackson, S.E., Pearson, N.J., Griffin, W.L., Belousova, E.A., 2004, The application of laser ablation-inductively coupled plasma-mass spectrometry to in situ U–Pb zircon geochronology. Chemical Geology 211, 47-69.

Jacobsen, S.B., Wasserburg, J.G., 1980. Sm-Nd isotopic evolution of chondrites. Earth & Planetary Science Letters 50, 139-155.

Kamenetsky V. S., Sobolev A. V., Eggins S. M., Crawford A. J. and Arculus R. J., 2002. Olivine-enriched melt inclusions in chromites from low-Ca boninites, Cape Vogel, Papua New Guinea: evidence for ultramafic primary magma, refractory mantle source and enriched components. Chemical Geology 183(1-4), 287-303.

Kessel R., Schmidt M.W., Ulmer P. and Pettke T. 2005. Trace element signature of subduction-zone fluids, melts and supercritical liquids at 120–180 km depth. Nature 437, 29, doi:10.1038/nature03971

Kimura, J.-I., Hacker B. R., van Keken P. E., Kawabata H., Yoshida T., and Stern R. J. 2009. Arc Basalt Simulator version 2, a simulation for slab dehydration and fluid-fluxed mantle melting for arc basalts: Modeling scheme and application, Geochemistry, Geophysics, Geosystems, 10, Q09004, doi:10.1029/2008GC002217.

Kimura, J.-I., A. J. R. Kent, M. C. Rowe, M. Katakuse, F. Nakano, B. R. Hacker, P. E. van Keken, H. Kawabata, and R. J. Stern, 2010. Origin of cross-chain geochemical variation in Quaternary lavas from the northern Izu arc: Using a quantitative mass balance approach to identify mantle sources and mantle wedge processes, Geochemistry, Geophysics, Geosystems, 11, Q10011, doi:10.1029/2010GC003050.

König S., Münker C., Schuth S., Luguet A., Hoffmann J.E., Kuduon J., 2010. Boninites as windows into trace element mobility in subduction zones. Geochimica et Cosmochimica Acta 74, 684–704. doi:10.1016/j.gca.2009.10.011

Kosler, J., 2001, Laser-ablation ICPMS study of metamorphic minerals and processes. In: Sylvester P. J. ed. Laser-ablation-ICPMS in the earth sciences; principles and applications Mineralogical Association of Canada Short Course Handbook 29, 185-202.

Kroenke L.W., 1972. Geology of the Ontong Java Plateau. PhD thesis, Hawaii Inst. of Geophysics Honolulu, 134p.

Leng, W., Gurnis, M., Asimow, P., 2012. From basalts to boninites: The geodynamics of volcanic expression during induced subduction initiation. Lithosphere 4, 511–523. doi:10.1130/L215.1

Li Y.B., Kimura J.I., Machida S., Ishii T., Ishiwatari A., Maruyama S., Qiu H.N., Ishikawa T., Kato Y., Haraguchi S., Takahata N., Hirahara Y. and Miyazaki T., 2013. High-Mg adakite and low-Ca Boninite from a Bonin fore-arc seamount: implications for the reaction between slab melts and depleted mantle. Journal of Petrology 54 (6): 1149-1175. doi:10.1093/petrology/egt008

Ludwig, K.R., 2003. User's Manual for Isoplot 3.00 a Geochronological Toolkit for Microsoft Excel.

Macpherson, C.G. and Hall, R., 2001. Tectonic Setting of Eocene Boninite Magmatism in the Izu-Bonin-Mariana Forearc, Earth & Planetary Science Letters 186, 215-230.

Marchesi C., Garrido C.J., Godard M., Belley F., and Ferré E., 2009. Migration and accumulation of ultra-depleted subduction-related melts in the Massif du Sud ophiolite (New Caledonia). Chemical Geology 266, 171-186.

Maurizot and Vendé-Leclerc, 2009. 1:500,000 Geological map of New Caledonia, Geological Survey, Government of New Caledonia (www.georep.nc)

Maurizot P. and Cluzel D. 2014. Pre-obduction records of Eocene foreland basins in central New Caledonia (Southwest Pacific); an appraisal from surface geology and Cadart 1 borehole data. New Zealand Journal of Geology and Geophysics 57, 3, 307-311. doi:10.1080/00288306.2014.885065

Maurizot P., 2011. Premiers enregistrements sédimentaires de la convergence pré-obduction en Nouvelle-Calédonie : Formation d'un complexe d'accrétion à l'Eocène inférieur dans le Nord de la Grande-Terre et mise en place de la nappe des Montagnes Blanches, *Bulletin de la Société Géologique de France* 182, 479-491, doi:10.2113/gssgfbull.182.6.479.

McDade, P., Blundy, J.D., Wood, B.J., 2003. Trace element partitioning on the Tinaquillo Lherzolite solidus at 1.5GPa. Physics of the Earth and Planetary Interiors 139, 129–147. doi:10.1016/S0031-9201(03)00149-3

McDonough, W., Sun, S., 1995. The composition of the Earth. Chemical Geology 120, 223–253.

Ohnenstetter, D., Brown, W.L., 1992. Overgrowth textures, disequilibrium zoning, and cooling history of a glassy four-pyroxene boninite dike from New Caledonia. Journal of Petrology 33, 231–271.

Ohnenstetter, D., Brown, W.L., 1996. Compositional variation and primary water contents of differentiated interstitial and included glasses in boninites. Contributions to Mineralogy and Petrology 123, 117–137.

Pearce J. A. 1982. Trace element characteristics of lavas from destructive plate margins. In Thorpe R. S. (ed.). Andesites, pp. 528–548. John Wiley, Winchester.

Pearce, J. A., Lann, S. R.,Arculus, R. J., Murton, B. J., Ishii,T., Peate, D. W. and Parkinson, I. J. 1992a. Boninite and harzburgite from Leg 125 (Bonin-Mariana fore-arc): A case study of magma genesis during the initial stages of subduction. In: Fryer, P., Peace, J. A. & Stokking, L.B. (eds) Proceedings of the Ocean Drilling Program, Scientific Results, 125. College Station, TX: Ocean Drilling Program, pp. 623-659.

Pearce, J.A., Thirlwall, M.F., Ingram, G., Murton, B.J., Arculus, R.J., van der Laan, S.R., 1992b. Isotopic evidence for the origin of boninites and related rocks drilled in the Izu-Bonin (Ogasawara) fore arc, LEG 125. Proceedings of Ocean Drilling Program, Scientific Results 125, 237–261.

Pin, C. and Santos Zalduegui, J.F., 1997. Sequential separation of light rare-earth elements, thorium and uranium by miniaturized extraction chromatography ; application to isotopic analyses of silicate rocks. Analytica Chimica Acta 339, 79-89.

Pirard C., Hermann J. and O'Neill H., 2013. Petrology and geochemistry of the crust–mantle boundary in a nascent arc, Massif du Sud Ophiolite, New Caledonia, SW Pacific. Journal of Petrology 54 (9), 1759-1792. doi: 10.1093/petrology/egt030

Poli, S., and Schmidt, M.W. 2002. Petrology of subducted slabs. Annual Review of Earth and Planetary Sciences 30: 207-235. DOI: 10.1146/annurev.earth.30.091201.140550

Prinzhofer A. and Allègre, C. J., 1985. Residual peridotites and the mechanisms of partial melting. Earth and Planetary Science Letters 74, 251-265.

Prinzhofer, A., 1987. Structure et pétrologie d'un cortège ophiolitique: le massif du Sud (Nouvelle-Calédonie), Thèse Ing.-Doct. E.N.S.M.P., University Paris VII, 244pp.

Reagan M.K., Ishizuka O., Stern R.J., Kelley K.A., Ohara Y., et al., 2010. Fore-arc basalts and subduction initiation in the Izu-Bonin-Mariana system. Geochemistry, Geophysics, Geosystems 11, Q03X12. doi:10.1029/2009GC002871

Reagan M.K., McClelland W.C., Girard G., Goff K.R., Peate D. W., Ohara Y., Stern R. J. 2013. The geology of the southern Mariana fore-arc crust: Implications for the scale of Eocene volcanism in the Western Pacific. Earth and Planetary Science Letters 380, 41-51

Robinson, J.A.C., Wood, B.J., Blundy, J.D., 1998. The beginning of melting of fertile and depleted peridotite at 1.5GPa. Earth and Planetary Science Letters 155, 97–111.

Sack, P.J., Berry, R.F., Meffre, S., Falloon, T.J., Gemmell, J.B., Friedman, R.M., 2011. In situ location and U-Pb dating of small zircon grains in igneous rocks using laser ablation-inductively coupled plasma-quadrupole mass spectrometry. Geochemistry, Geophysics, Geosystems 12.

Sameshima T., Paris J.P., Black, P.M. and Heming R.F., 1983. Clinoenstatite-bearing lava from Népoui, New Caledonia. American Mineralogist 68, 1076-1082

Secchiari A. In prep. Geochemical characterization of New Caledonia ophiolite in the geodynamic framework of the Southwest Pacific; PhD co-tutelle thesis University of Parma (Italy), University of Montpellier 2 (France).

Secchiari A., Montanini A.; Bosch D.; Macera P.; Cluzel D. Melt extraction and enrichment processes in the New Caledonia lherzolites: evidence from geochemical and Sr-Nd isotope data. submitted to Lithos.

Shaw, D., 1970. Trace element fractionation during anatexis. Geochimica Cosmochimica Acta 34, 331–340.

Slama, J., Kosler, J., Condon, D.J., Crowley, J.L., Gerdes, A., Hanchar, J.M., Horstwood, M.S.A., Morris, G.A., Nasdala, L., Norberg, N., Schaltegger, U., Schoene, B., Tubrett, M.N., Whitehouse, M.J., 2008. Plesovice zircon - A new natural reference material for U-Pb and Hf isotopic microanalysis. Chemical Geology 249, 1-35.

Sobolev A.V., Danyushevsky L.V. 1994. Petrology and geochemistry of boninites from the north termination of the Tonga Trench: constraints on the generation conditions of primary high-Ca boninite magmas. Journal of Petrology 35, 1183–1211.

Solovova I.P., Ohnenstetter D., and Girnisa A.V., 2012. Melt inclusions in olivine from the boninites of New Caledonia: Post-entrapment melt modification and estimation of primary magma compositions. Petrology 20, 6, 529–544.

Spandler C. and Pirard C. 2013. Element recycling from subducting slabs to arc crust: A review. Lithos 170-171, 208-223.

Spandler C., Rubatto D. and Hermann, J., 2005, Late Cretaceous-Tertiary tectonics of the southwest Pacific: Insights from U-Pb sensitive, high resolution ion microprobe (SHRIMP) dating of eclogite facies rocks from New Caledonia: Tectonics, v. 24, TC3003. doi:10.1029/2004TC001709

Stern, R.J., Reagan, M., Ishizuka, O., Ohara, Y. and Whattam, S., 2012. To understand subduction initiation, study forearc crust; to understand forearc crust, study ophiolites. Lithosphere 4, 469–483.

Thorkelson, D.J., and Breitsprecher, K., 2005, Partial melting of slab window margins: Genesis of adakitic and non-adakitic magmas: Lithos 79, 25-41, doi: 10.1016/j.lithos.2004.04.049.

Tiepolo M., Vannucci R., Oberti R., Foley S., Bottazzi P. and Zanetti A., 2000. Nb and Ta incorporation and fractionation in titanian pargasite and kaersutite: crystal chemical constraints and implications for natural systems. Earth and Planetary Science Letters 176(2), 185-201.

Ulrich M., Picard C., Guillot S., Chauvel C., Cluzel D. and Meffre S., 2010. Multiple melting stages and refertilisation process as indicators for ridge to subduction formation: the New Caledonia Ophiolite, Lithos 115, 223-236.

Umino S. and Kushiro I. 1989. Experimental studies on boninite petrogenesis. In: Crawford, A. J. (ed.) Boninite and Related Rocks. London: Unwin Hyman, pp. 89-109.

Van der Laan, S. R., Flower, M. F. J. & Koster Van Groos, A. K. 1989. Experimental evidence for the origin of boninites: near-liquidus phase relations to 7·5 kbar. In: Crawford, A. J. (ed.) Boninite and Related Rocks. London: Unwin Hyman, pp. 112-147.

Wiedenbeck, M., Alle, P., Corfu, F., Griffin W.L., Meier, M., Oberli, F., Vonquadt A., Roddick, J.C., Speigel W., 1995. 3 Natural Zircon Standards for U-Th-Pb, Lu-Hf, Trace-Element and REE Analyses. Geostandards Newsletter 19, 1-23.

Workman R.K. and Hart S. R., 2005. Major and trace element composition of the depleted MORB mantle (DMM). Earth and Planetary Science Letters 23, 11-2, 53-72. doi:10.1016/j.epsl.2004.12.005

Fig. 1

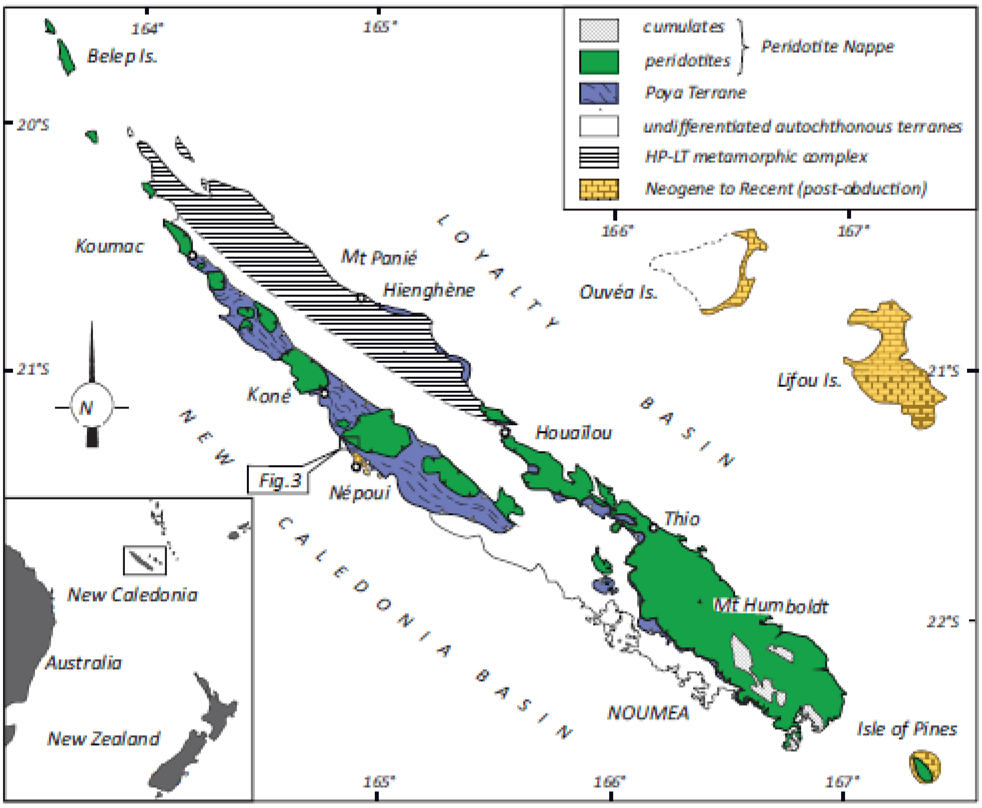
cumulates
peridotites
Peridotite Nappe
Poya Terrane
undifferentiated autochthonous terranes
HP-LT metamorphic complex
Neogene to Recent (post-obduction)
164°
165°
166°
167°
20°S
21°S
22°S
Belep Is.
Koumac
Mt Panié
Hienghène
LOYALTY BASIN
Ouvéa Is.
Lifou Is.
Koné
Fig.3
Népoui
Houaïlou
Thio
Mt Humboldt
NOUMEA
Isle of Pines
NEW CALEDONIA BASIN
N
New Caledonia
Australia
New Zealand

Fig. 2

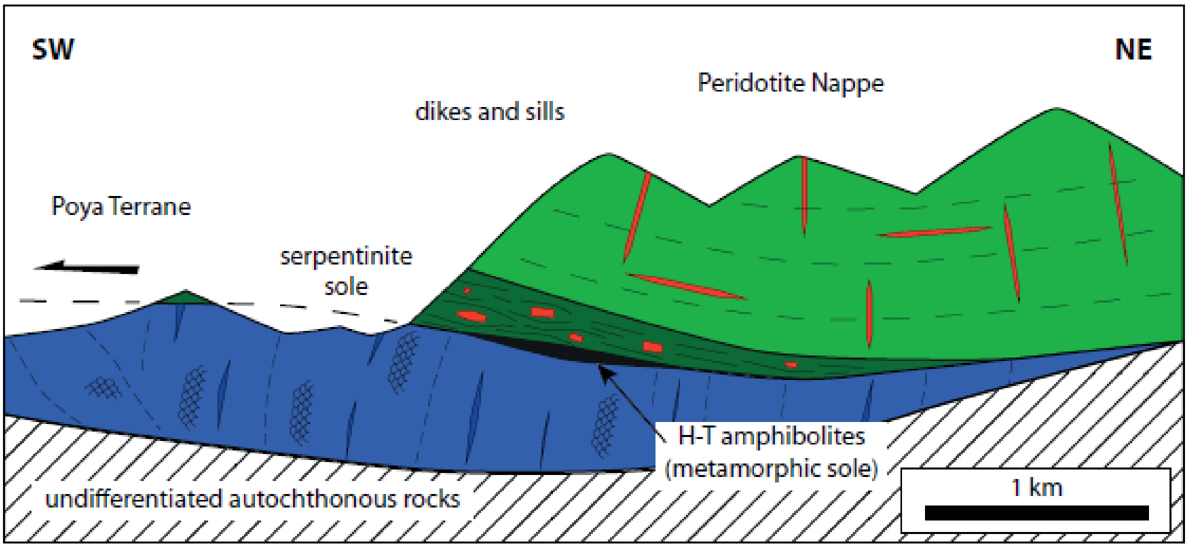
SW
NE
Peridotite Nappe
dikes and sills
Poya Terrane
serpentinite
sole
H-T amphibolites
(metamorphic sole)
1 km
undifferentiated autochthonous rocks

Fig. 3

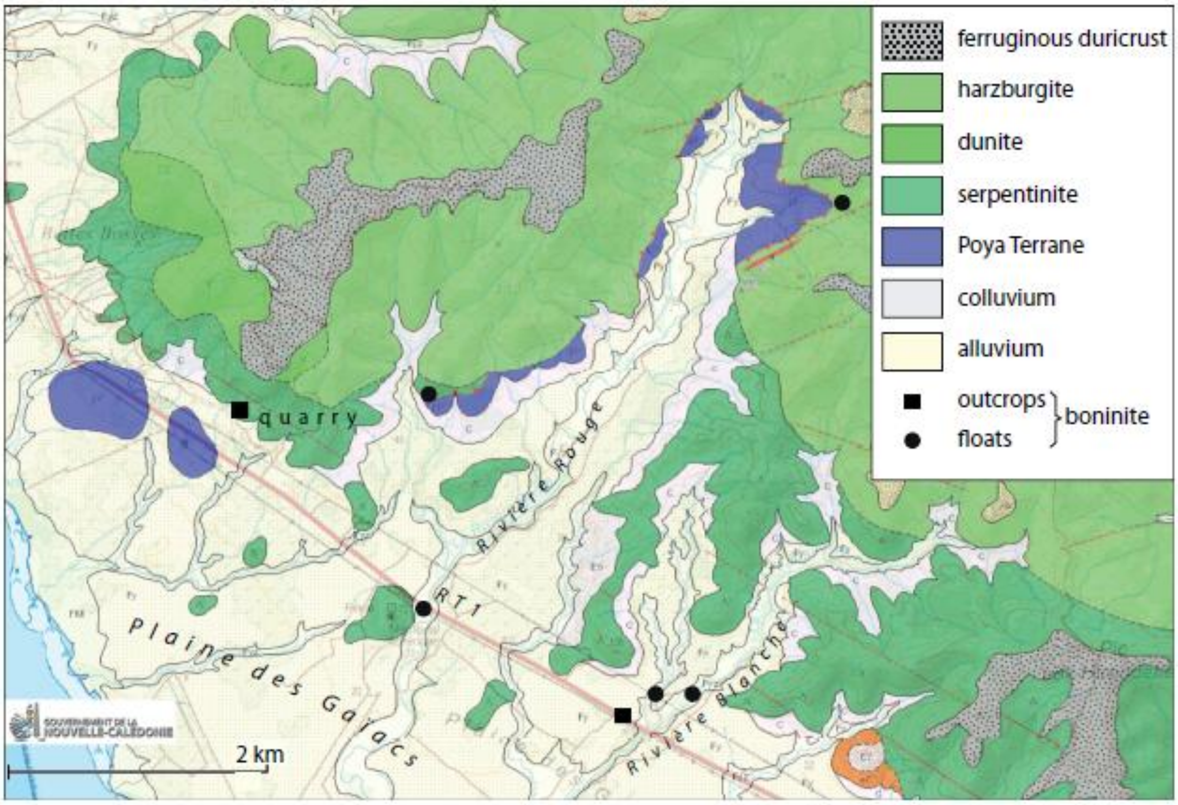
ferruginous duricrust
harzburgite
dunite
serpentinite
Poya Terrane
colluvium
alluvium
outcrops
floats
boninite
quarry
Rivière Rouge
RT1
Plaine des Gaïacs
Rivière Blanche
2 km

Fig. 4

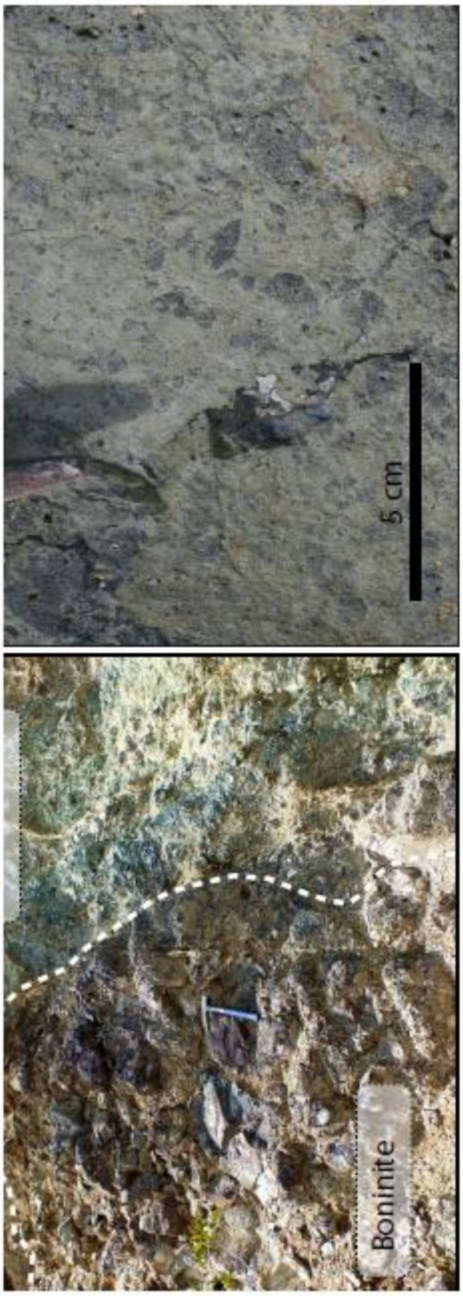

Fig. 5

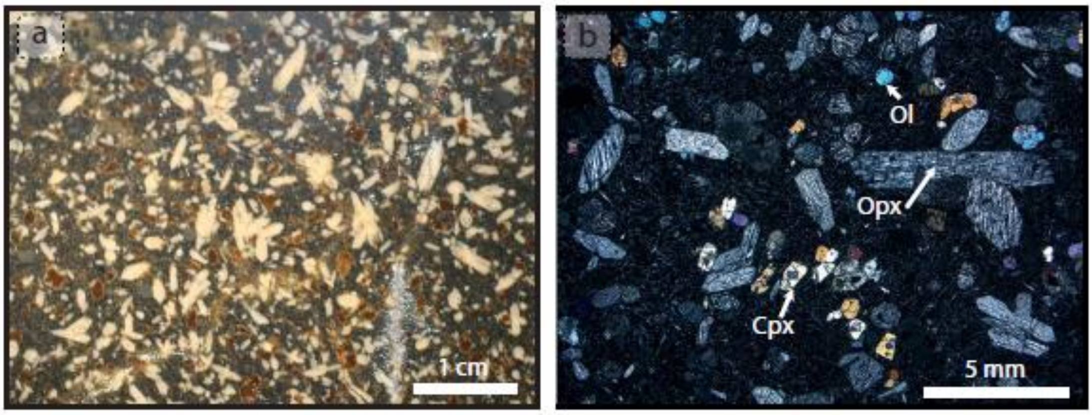

Fig. 6

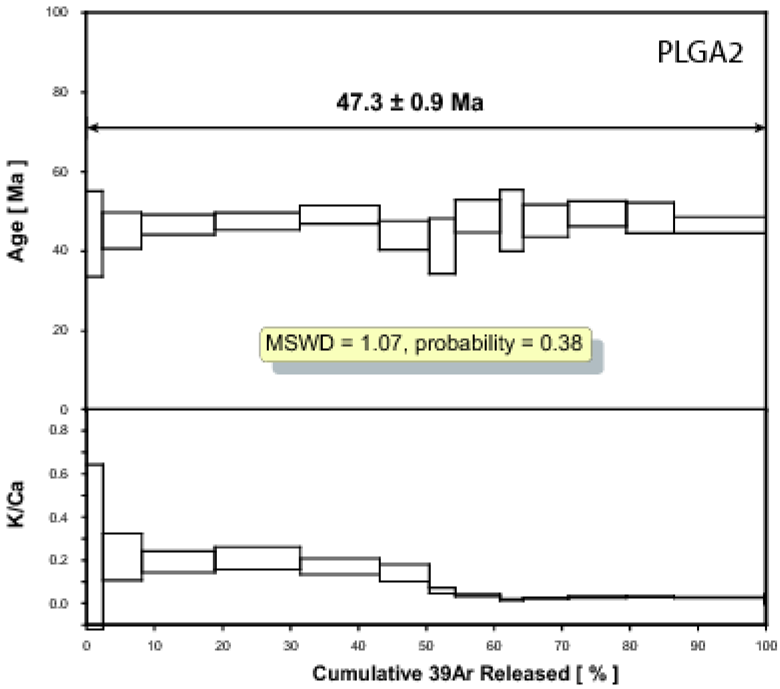

PLGA2
47.3 ± 0.9 Ma
MSWD = 1.07, probability = 0.38
Age [Ma]
K/Ca
Cumulative 39Ar Released [%]

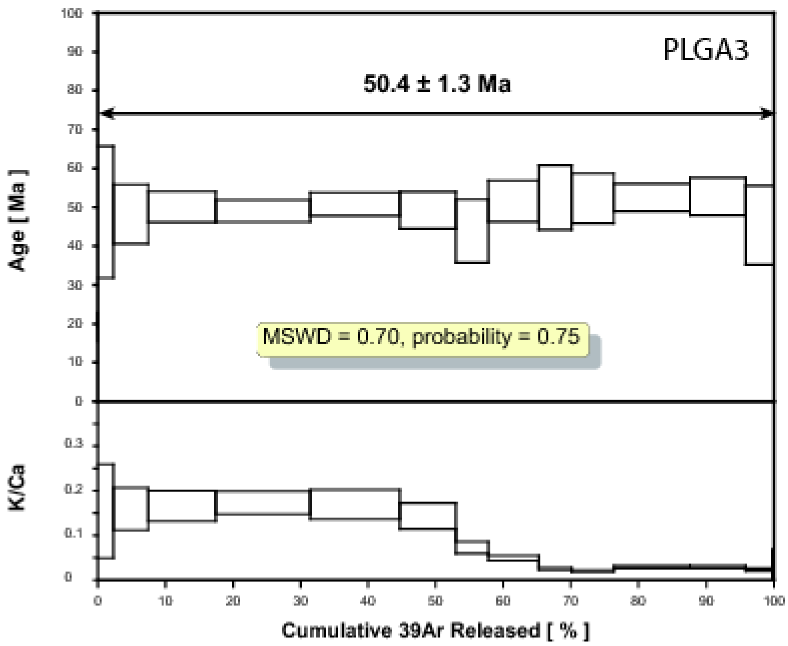

PLGA3
50.4 ± 1.3 Ma
MSWD = 0.70, probability = 0.75
Age [Ma]
K/Ca
Cumulative 39Ar Released [%]

Fig. 7

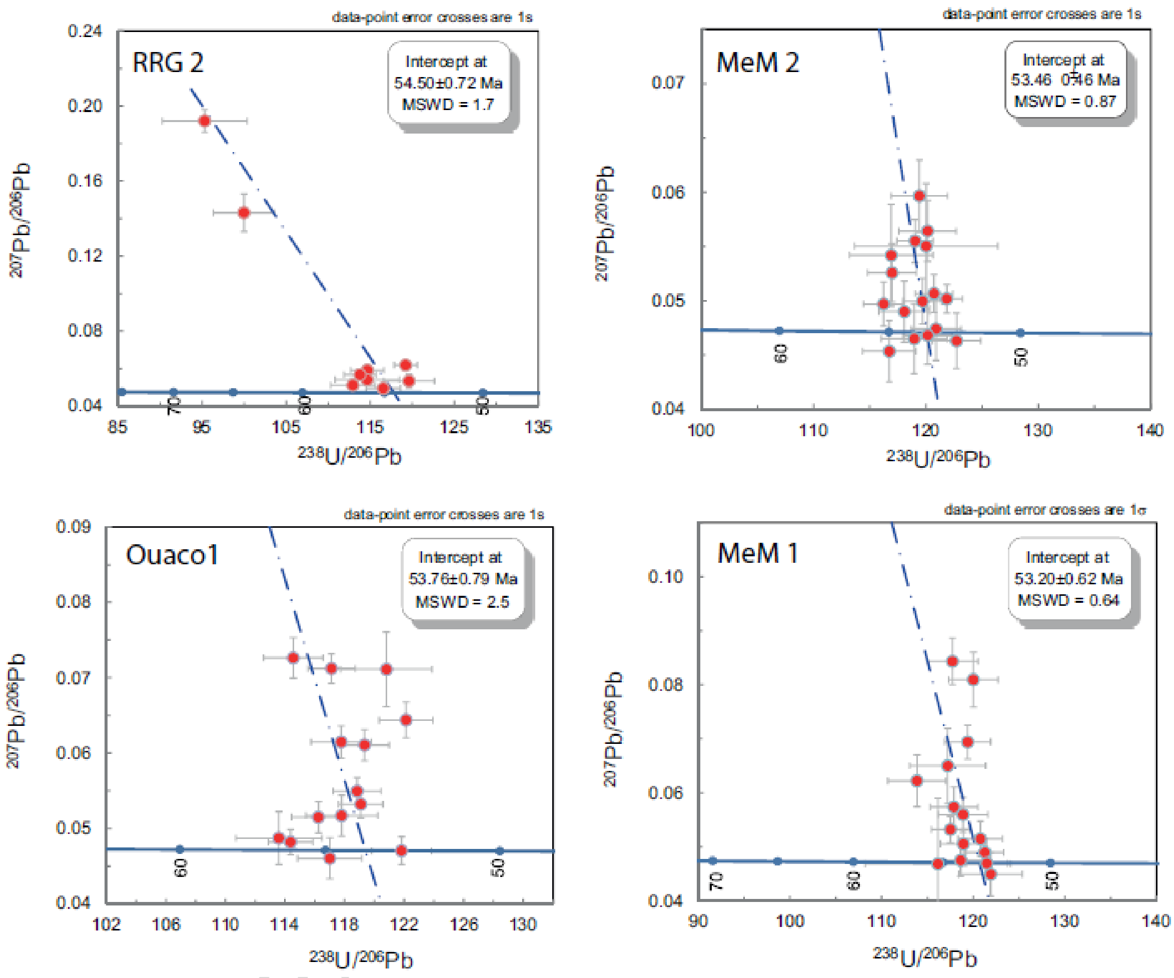

data-point error crosses are 1s
RRG 2
Intercept at
54.50±0.72 Ma
MSWD = 1.7
$^{207}Pb/^{206}Pb$
$^{238}U/^{206}Pb$
data-point error crosses are 1s
MeM 2
Intercept at
53.46 0.46 Ma
MSWD = 0.87
data-point error crosses are 1s
Ouaco1
Intercept at
53.76±0.79 Ma
MSWD = 2.5
data-point error crosses are 1σ
MeM 1
Intercept at
53.20±0.62 Ma
MSWD = 0.64

Fig. 8

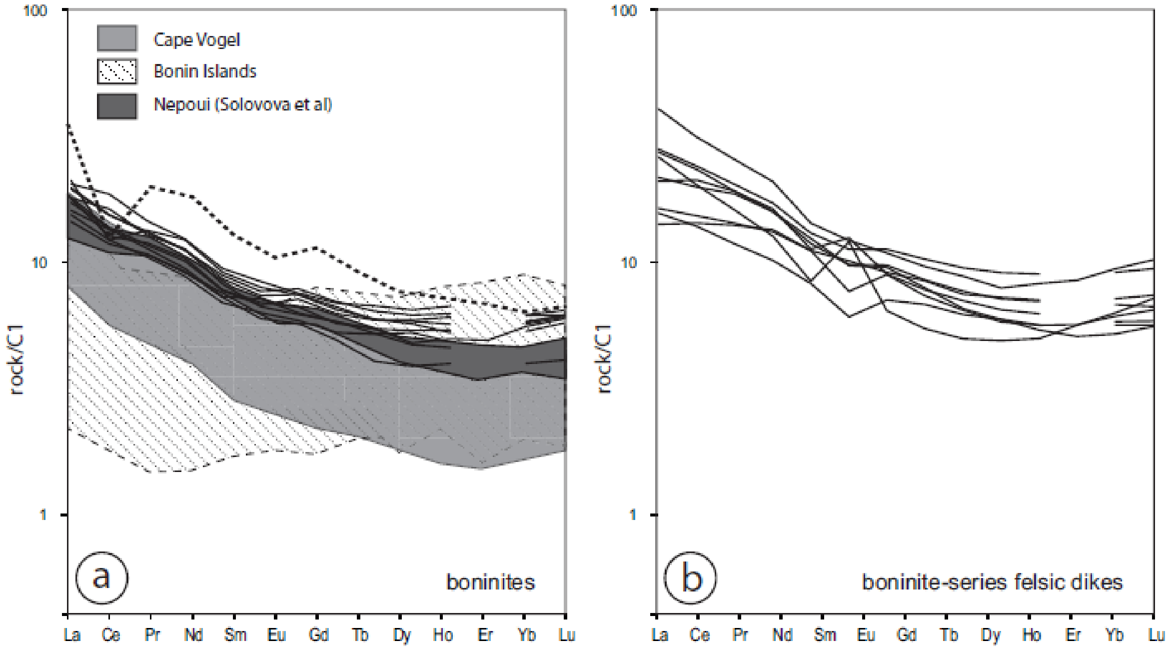
100
10
1
rock/C1
Cape Vogel
Bonin Islands
Nepoui (Solovova et al)
a
boninites
La Ce Pr Nd Sm Eu Gd Tb Dy Ho Er Yb Lu
100
10
1
rock/C1
b
boninite-series felsic dikes
La Ce Pr Nd Sm Eu Gd Tb Dy Ho Er Yb Lu

Fig. 9

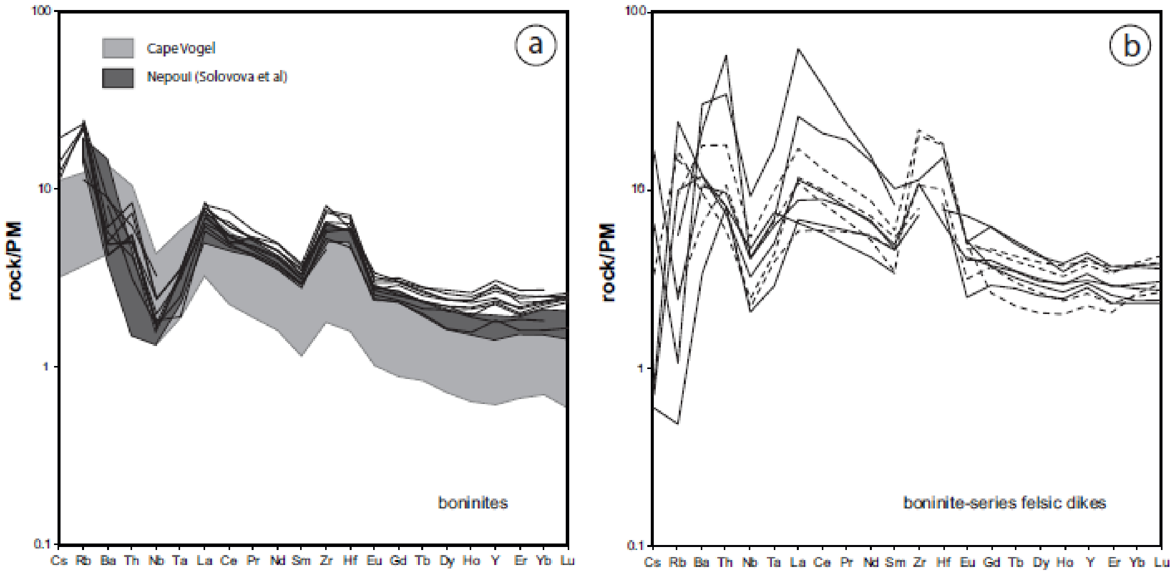

100
10
1
0.1
rock/PM
Cape Vogel
Nepoui (Solovova et al)
a
boninites
Cs Rb Ba Th Nb Ta La Ce Pr Nd Sm Zr Hf Eu Gd Tb Dy Ho Y Er Yb Lu
b
boninite-series felsic dikes

Fig. 10

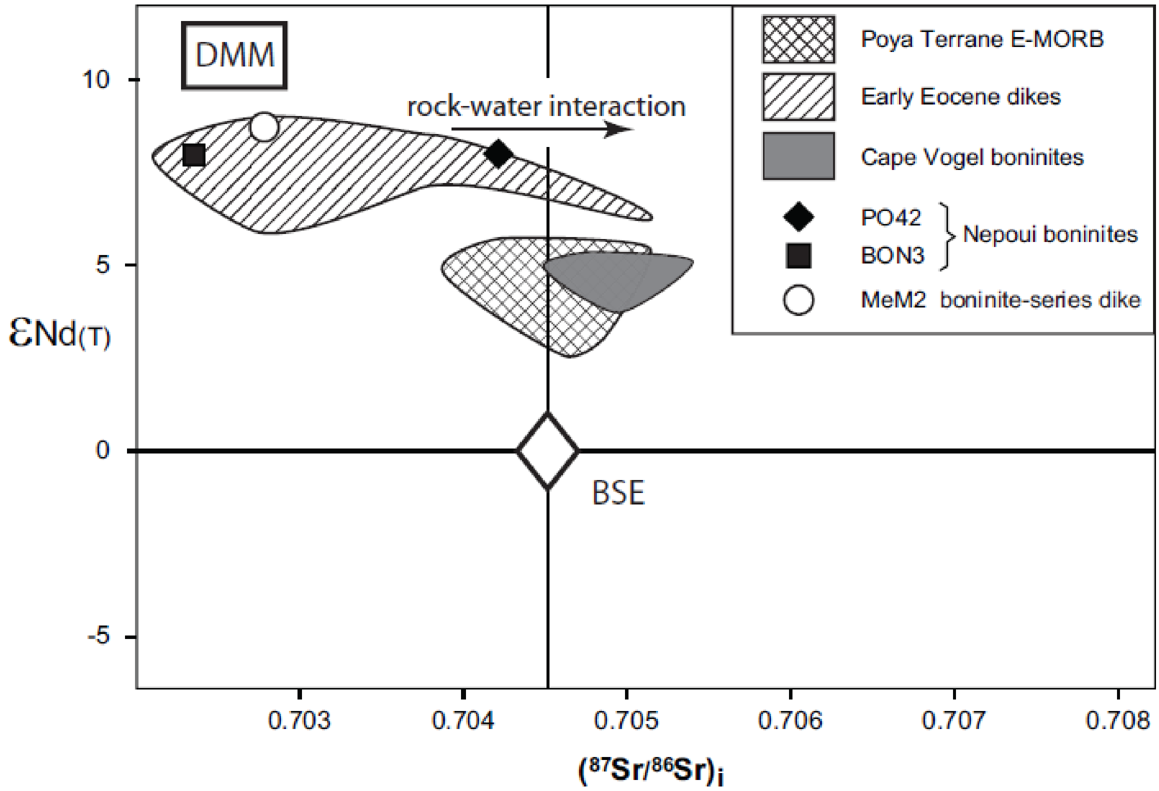
DMM
rock-water interaction
BSE
10
5
0
-5
ƐNd(T)
0.703
0.704
0.705
0.706
0.707
0.708
(^{87}Sr/^{86}Sr)$_i$
Poya Terrane E-MORB
Early Eocene dikes
Cape Vogel boninites
PO42
BON3
Nepoui boninites
MeM2 boninite-series dike

Fig. 11

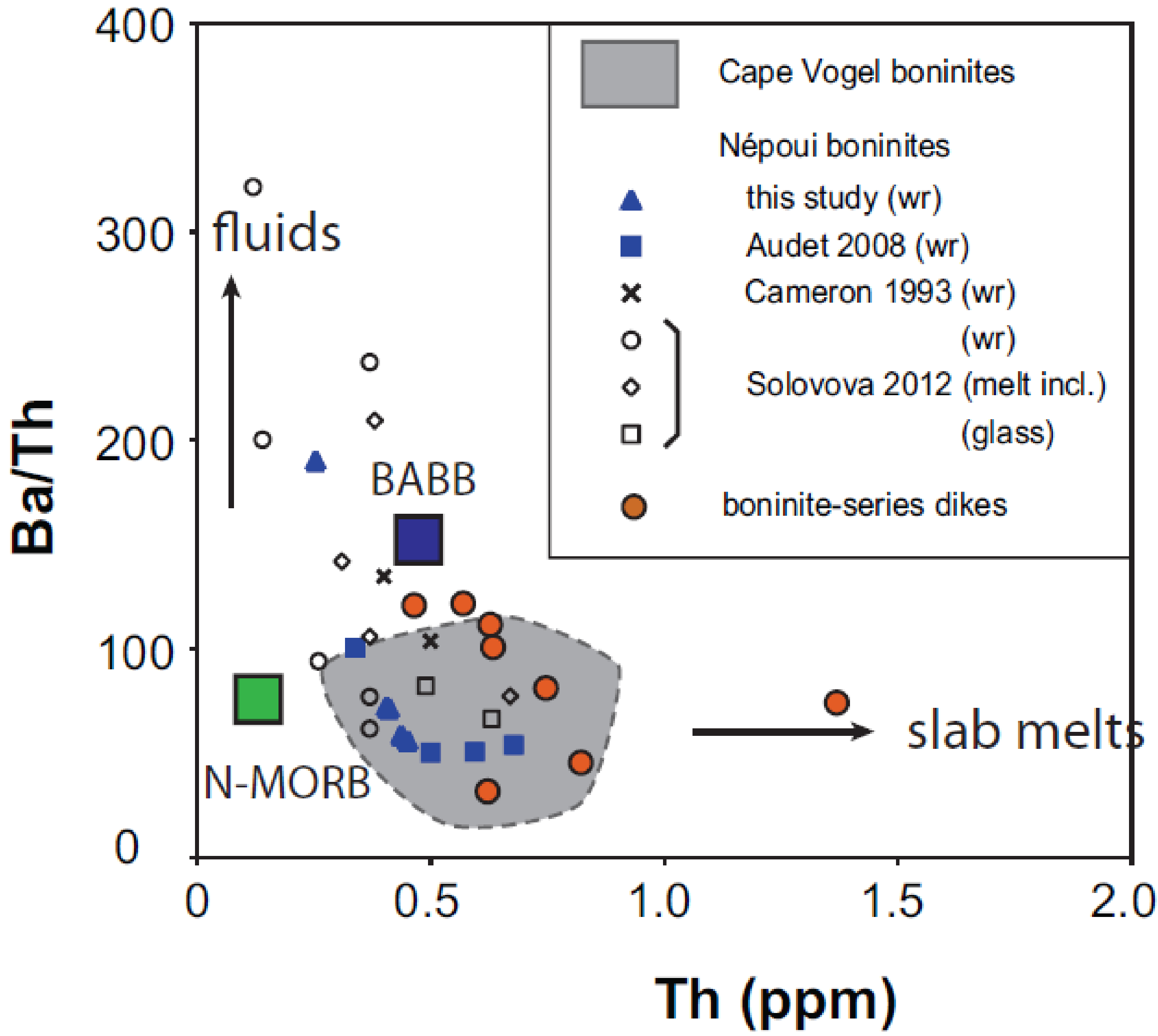

400
300
200
100
0
Ba/Th
fluids
BABB
N-MORB
slab melts
0
0.5
1.0
1.5
2.0
Th (ppm)
Cape Vogel boninites
Népoui boninites
this study (wr)
Audet 2008 (wr)
Cameron 1993 (wr)
(wr)
Solovova 2012 (melt incl.)
(glass)
boninite-series dikes

Fig. 12

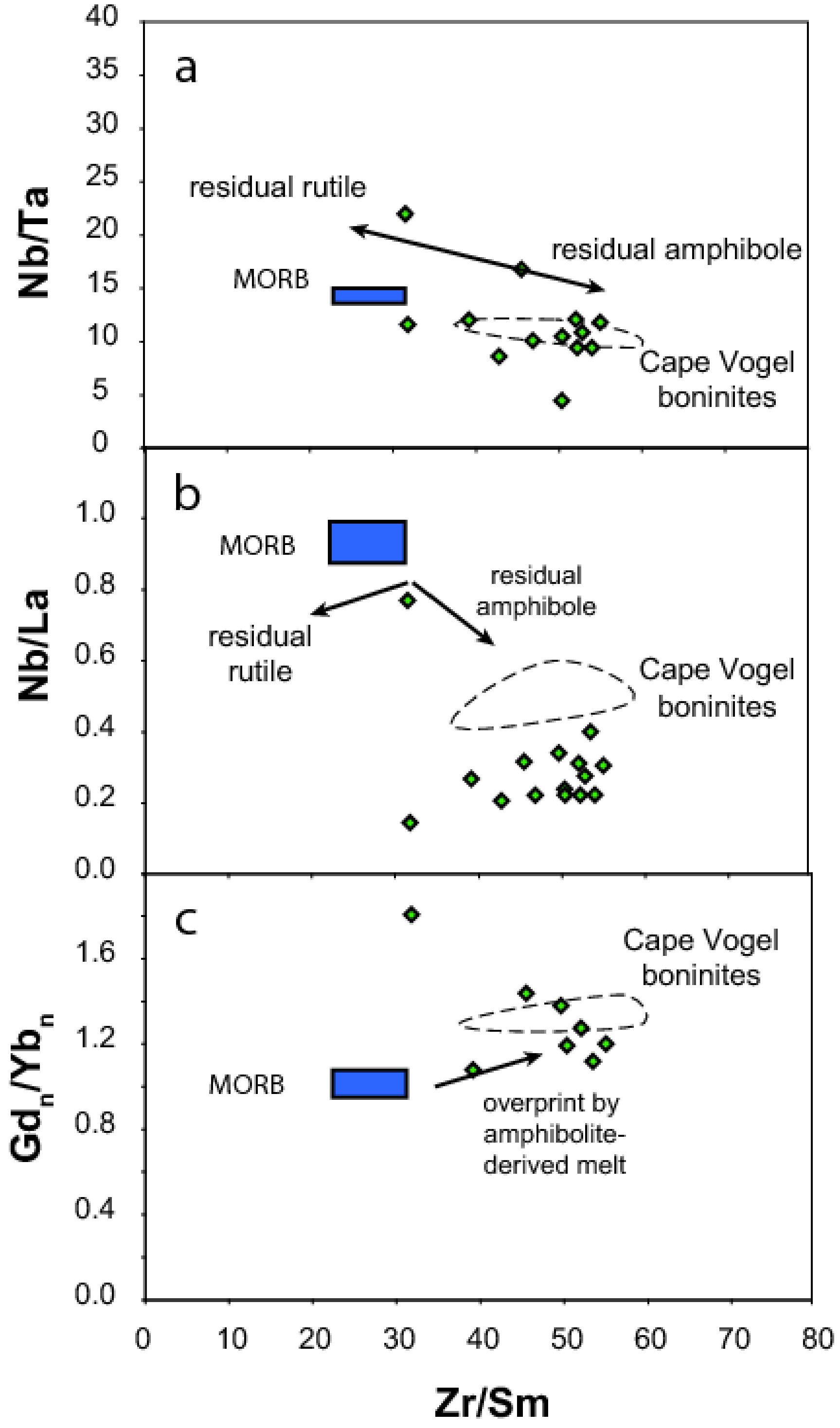
a
b
c
Nb/Ta
Nb/La
Gd$_n$/Yb$_n$
Zr/Sm
residual rutile
residual amphibole
MORB
Cape Vogel
boninites
residual
amphibole
residual
rutile
overprint by
amphibolite-
derived melt
0
5
10
15
20
25
30
35
40
0.0
0.2
0.4
0.6
0.8
1.0
0.4
0.8
1.2
1.6
0
10
20
30
40
50
60
70
80

Fig. 13

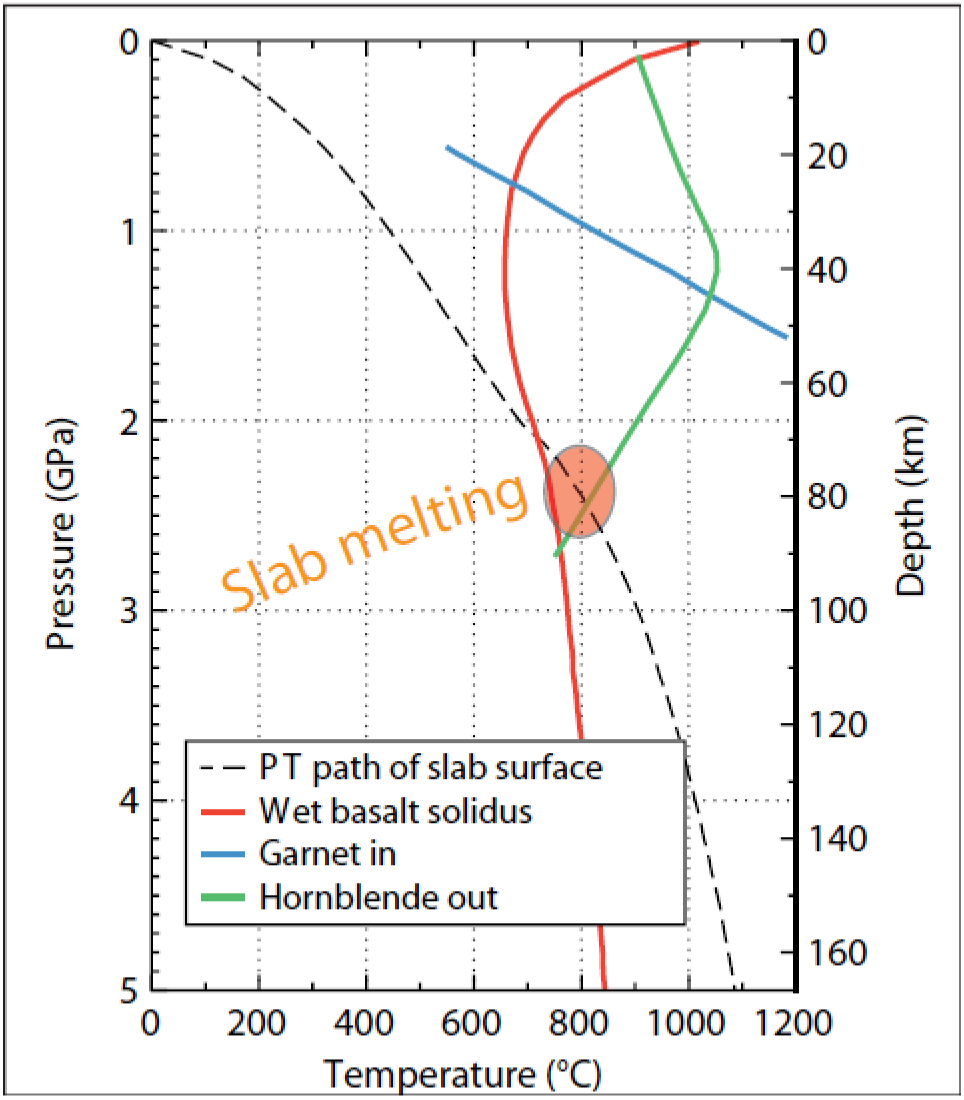

0
1
2
3
4
5
Pressure (GPa)
0
20
40
60
80
100
120
140
160
Depth (km)
0
200
400
600
800
1000
1200
Temperature (°C)
Slab melting
PT path of slab surface
Wet basalt solidus
Garnet in
Hornblende out

Fig. 14

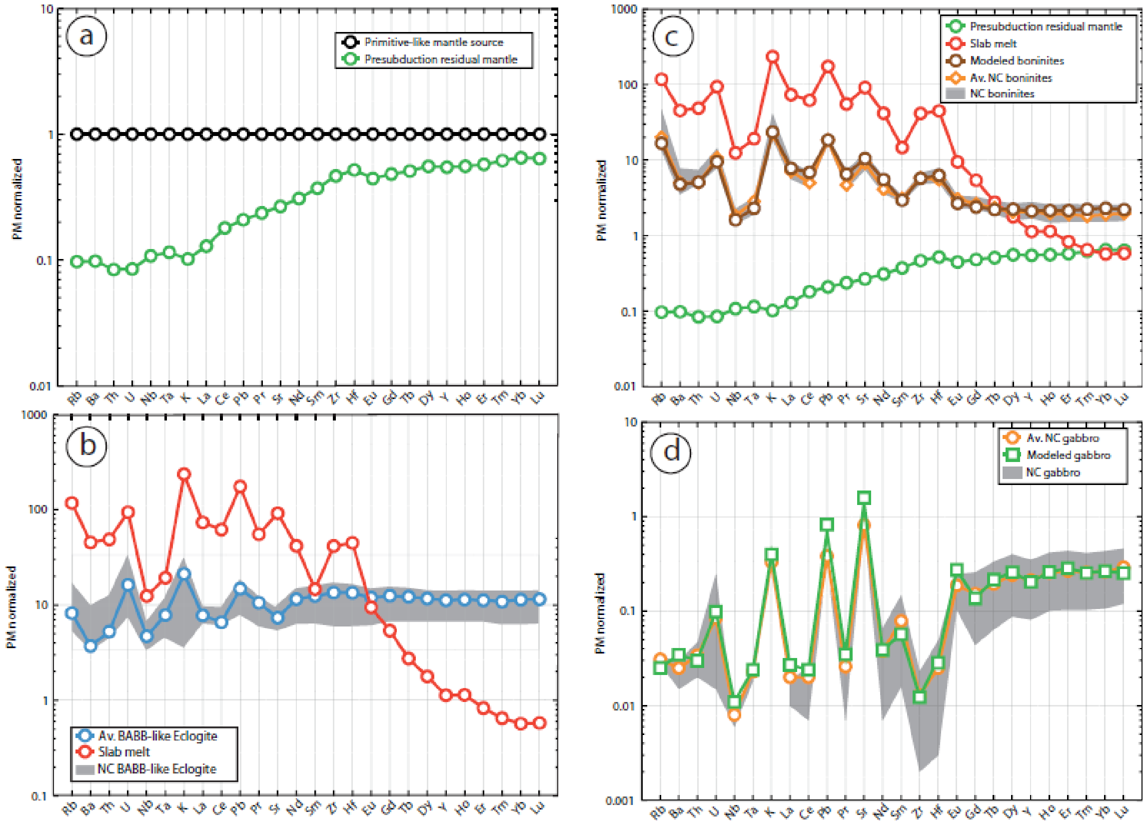
a
Primitive-like mantle source
Presubduction residual mantle
PM normalized
b
Av. BABB-like Eclogite
Slab melt
NC BABB-like Eclogite
c
Presubduction residual mantle
Slab melt
Modeled boninites
Av. NC boninites
NC boninites
d
Av. NC gabbro
Modeled gabbro
NC gabbro
Rb Ba Th U Nb Ta K La Ce Pb Pr Sr Nd Sm Zr Hf Eu Gd Tb Dy Y Ho Er Tm Yb Lu

Fig. 15

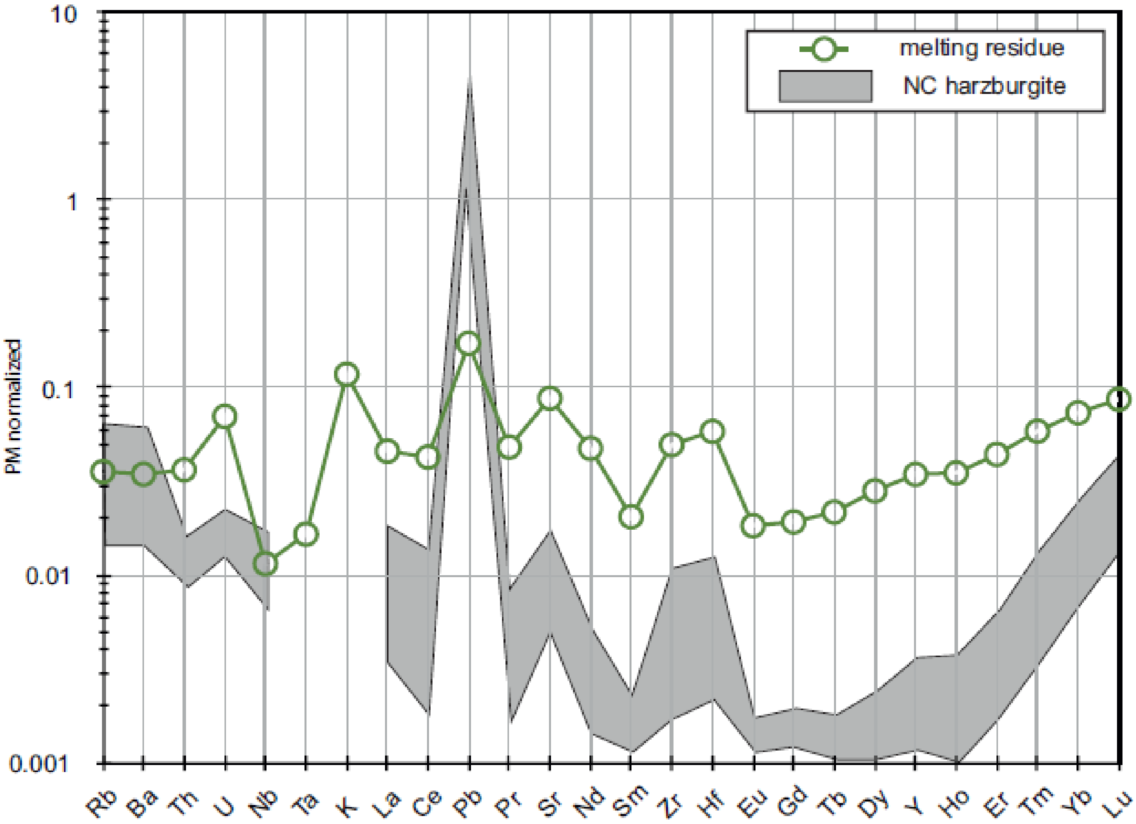
melting residue
NC harzburgite
PM normalized
10
1
0.1
0.01
0.001
Rb
Ba
Th
U
Nb
Ta
K
La
Ce
Pb
Pr
Sr
Nd
Sm
Zr
Hf
Eu
Gd
Tb
Dy
Y
Ho
Er
Tm
Yb
Lu

Fig. 16

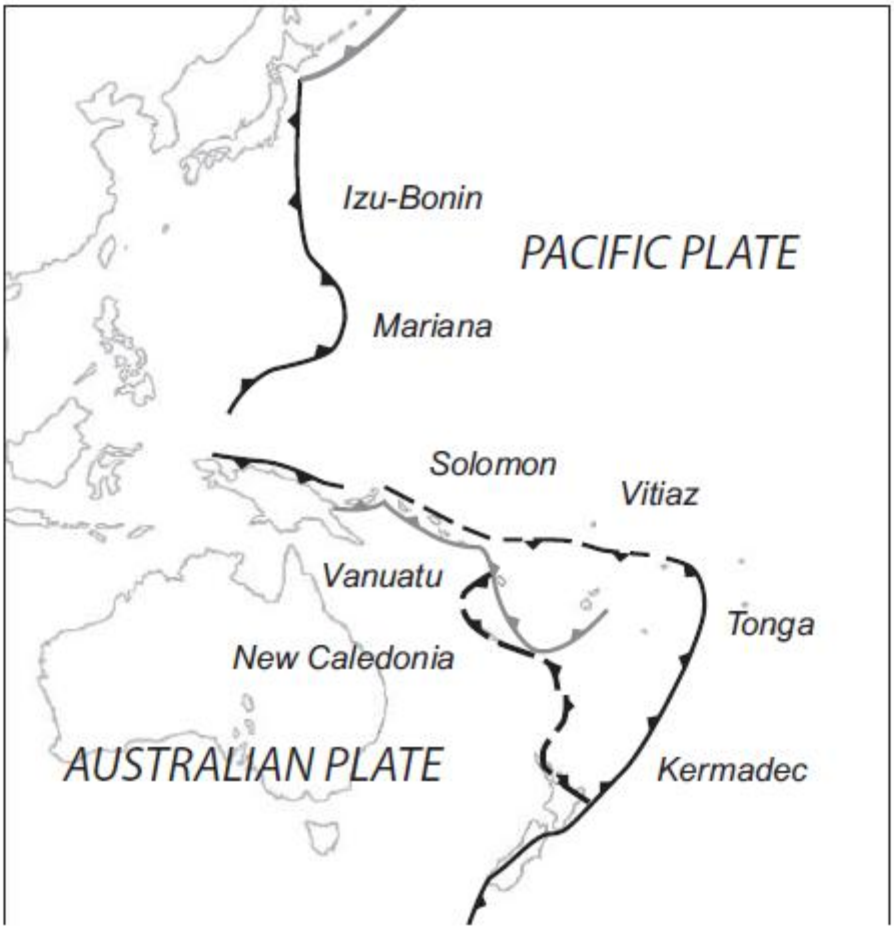
Izu-Bonin
PACIFIC PLATE
Mariana
Solomon
Vitiaz
Vanuatu
Tonga
New Caledonia
AUSTRALIAN PLATE
Kermadec

Fig. 17

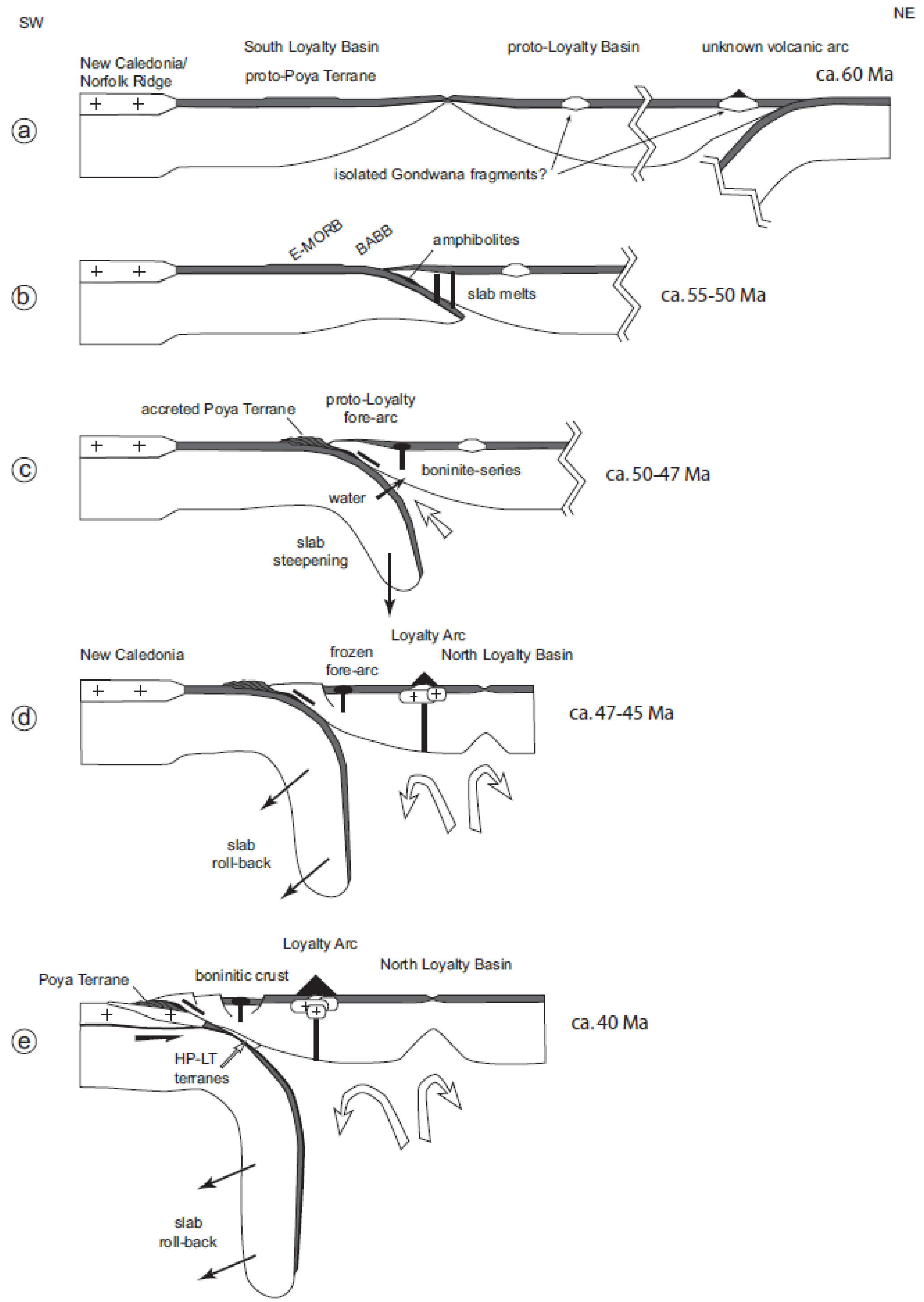
SW
NE
New Caledonia/
Norfolk Ridge
South Loyalty Basin
proto-Poya Terrane
proto-Loyalty Basin
unknown volcanic arc
ca. 60 Ma
ⓐ
isolated Gondwana fragments?
E-MORB
BABB
amphibolites
ⓑ
slab melts
ca. 55-50 Ma
accreted Poya Terrane
proto-Loyalty
fore-arc
ⓒ
boninite-series
ca. 50-47 Ma
water
slab
steepening
New Caledonia
frozen
fore-arc
Loyalty Arc
North Loyalty Basin
ⓓ
ca. 47-45 Ma
slab
roll-back
Loyalty Arc
North Loyalty Basin
Poya Terrane
boninitic crust
ⓔ
ca. 40 Ma
HP-LT
terranes
slab
roll-back

Highlights

CE-boninite and boninite-series felsic dikes of New Caledonia yield Early Eocene $^{40}Ar/^{39}Ar$ and U-Pb zircon ages respectively.

Geochemical and isotopic features and geochemical modeling suggest source enrichment by subduction-derived fluids and MORB-like melt component.

Modeling also suggests that CE-boninite magma may have been in equilibrium with enstatite-bearing gabbro cumulates of the Peridotite Nappe that formed in the fore-arc region of the nascent Loyalty Arc